ИНФОРМАЦИЯ ЗА:
Наименование на заболяването
Паркинсоново-пирамиден синдром
Определение на заболяването
Паркинсон-пирамидният синдром обединява ювенилна парализа ажитанс на Hunt и PARK 15. Ювенилна парализа ажитанс на Hunt е с начало в юношеството или по-рано на типичен паркинсонизъм с тремор, масковиден фациес, брадикинезия, дизартрия, ригидност и понякога дистония. Прогресията на синдрома е много бавна. Субстанция нигра е нормална, но се наблюдава дегенерация и загуба на големи клетки на лентикуларните ядра. PARK 15 започва във второто и началото на трето десетилетие с картина парализа ажитанс и пирамидни белези. Постмортем изследванията показват избледняване на палдалния сегмент, изтъняване на анза лентикуларис, леко свиване и клетъчни промени в субстанция нигра и ранна демиелинизация на пирамидите и кръстосване на пирамидните трактове.
Четирицифрен код на заболяването по МКБ-10 (ако такъв е наличен)
G20
Код на заболяването по Orpha code
ORPHA171695
Епидемиологични данни за заболяването в Република България
<1/1 000 000; Точните заболеваемост и болестност са неизвестни. Предполага се заболеваемост и болестност сходна на останалите страни в Европа.
В т.ч. научни публикации от последните пет години и приложена библиографска справка
1. Milanov I, Kmetska K, Karakolev B, Nedialkov E. Prevalence of Parkinson's disease in Bulgaria. Neuroepidemiology. 2001;20(3):212-4. 2. Shojaee, S., Sina, F., Banihosseini, S. S., Kazemi, M. H., Kalhor, R., Shahidi, G.-A., Fakhrai-Rad, H., Ronaghi, M., Elahi, E. Genome-wide linkage analysis of a parkinsonian-pyramidal syndrome pedigree by 500 K SNP arrays. Am. J. Hum. Genet. 82: 1375-1384, 2008. 3. Di Fonzo, A., Dekker, M. C. J., Montagna, P., Baruzzi, A., Yonova, E. H., Correia Guedes, L., Szczerbinska, A., Zhao, T., Dubbel-Hulsman, L. O. M., Wouters, C. H., de Graaff, E., Oyen, W. J. G., Simons, E. J., Breedveld, G. J., Oostra, B. A., Horstink, M. W., Bonifati, V. FBXO7 mutations cause autosomal recessive, early-onset parkinsonian-pyramidal syndrome. Neurology 72: 240-245, 2009. 4. Zhao T, De Graaff E, Breedveld GJ, Loda A, Severijnen LA, Wouters CH, Verheijen FW, Dekker MC, Montagna P, Willemsen R, Oostra BA, Bonifati V. Loss of nuclear activity of the FBXO7 protein in patients with parkinsonianpyramidal syndrome (PARK15). PLoS One 2011;6:e16983. 5. Paisán-Ruiz C, Guevara R, Federoff M, Hanagasi H, Sina F, Elahi E, Schneider SA,

Schwingenschuh P, Bajaj N, Emre M, Singleton AB, Hardy J, Bhatia KP, Brandner S, Lees AJ, Houlden H. Early-onset L-dopa-responsive parkinsonism with pyramidal signs due to ATP13A2, PLA2G6, FBXO7 and spatacsin mutations. Mov Disord 2010;25:1791-1800.

Епидемиологични данни за заболяването в Европейския съюз

<1/1 000 000; Точните заболеваемост и болестност са неизвестни; До момента са описани 18 пациента от 5 семейства с хомозиготна или комбинирана хетерозиготна мутация на FBXO7 гена.

В т.ч. научни публикации от последните пет години и приложена библиографска справка

1. Shojaee, S., Sina, F., Banihosseini, S. S., Kazemi, M. H., Kalhor, R., Shahidi, G.-A., Fakhrai-Rad, H., Ronaghi, M., Elahi, E. Genome-wide linkage analysis of a parkinsonian-pyramidal syndrome pedigree by 500 K SNP arrays. Am. J. Hum. Genet. 82: 1375-1384, 2008.
2. Di Fonzo, A., Dekker, M. C. J., Montagna, P., Baruzzi, A., Yonova, E. H., Correia Guedes, L., Szczerbinska, A., Zhao, T., Dubbel-Hulsman, L. O. M., Wouters, C. H., de Graaff, E., Oyen, W. J. G., Simons, E. J., Breedveld, G. J., Oostra, B. A., Horstink, M. W., Bonifati, V. FBXO7 mutations cause autosomal recessive, early-onset parkinsonian-pyramidal syndrome. Neurology 72: 240-245, 2009.
3. Zhao T, De Graaff E, Breedveld GJ, Loda A, Severijnen LA, Wouters CH, Verheijen FW, Dekker MC, Montagna P, Willemsen R, Oostra BA, Bonifati V. Loss of nuclear activity of the FBXO7 protein in patients with parkinsonianpyramidal syndrome (PARK15). PLoS One 2011;6:e16983.
4. Paisán-Ruiz C, Guevara R, Federoff M, Hanagasi H, Sina F, Elahi E, Schneider SA, Schwingenschuh P, Bajaj N, Emre M, Singleton AB, Hardy J, Bhatia KP, Brandner S, Lees AJ, Houlden H. Early-onset L-dopa-responsive parkinsonism with pyramidal signs due to ATP13A2, PLA2G6, FBXO7 and spatacsin mutations. Mov Disord 2010;25:1791-1800.

Оценка на съответствието на заболяването с дефиницията за рядко заболяване съгласно § 1, т. 42 от допълнителните разпоредби на Закона за здравето

Заболяването е с разпространение под 5/ 10 000 души от населението на Европейския съюз.

Критерии за диагностициране на заболяването

Диагностициране на заболяването (дефиниция на случай):

Признаците и симптомите на заболяването: Ювенилна парализа ажитанс на Hunt е с начало в юношеството или по-рано на типичен паркинсонизъм с тремор, масковиден фациес, брадикинезия, дизартрия, ригидност и понякога дистония. Прогресията на синдрома е много бавна. PARK 15 започва във второто и началото на трето десетилетие с картина парализа ажитанс и пирамидни белези.

Етиологията и патогенезата: При ювенилна парализа ажитанс на Hunt субстанция нигра е нормална, но се наблюдава дегенерация и загуба на големи клетки на лентикуларните ядра. При PARK 15 постмортем изследванията показват избледняване на палдалния сегмент, изтъняване на анза лентикуларис, леко свиване и клетъчни промени в субстанция нигра и ранна демиелинизация на пирамидите и кръстосването на пирамидните трактове.

В т.ч. научни публикации от последните пет години и приложена библиографска справка

1. Ford, F. R. Hypertrophic interstitial poly-neuritis. Diseases of the Nervous System in Infancy, Childhood and Adolescence. (4th ed.) Springfield, Ill.: Charles C Thomas (pub.) 1961. Pp. 369-399.
2. Hunt, J. R. Progressive atrophy of the globus pallidus (primary atrophy of the pallidal system): a system disease of the paralysis agitans type, characterized by atrophy of the motor cells of the corpus striatum; a contribution to the functions of the corpus striatum. Brain 40: 58-148, 1917
3. Allen, N., Knopp, W. Hereditary parkinsonism-dystonia with sustained control by L-DOPA and anticholinergic medication. Adv. Neurol. 14: 201-213, 1976.
4. Martin, W. E., Resch, J. A., Baker, A. B. Juvenile parkinsonism. Arch. Neurol. 25: 494-500, 1971.
5. Davison, C. Pallido-pyramidal disease. J. Neuropath. Exp. Neurol. 13: 50-59, 1954.
6. Lange, E., Poppe, W. Klinischer Beitrag zum Krankheitsbild der progressiven Pallidumatrophie (van Bogaert). Psychiat. Neurol. (Basel) 146: 176-192, 1963.
7. Nisipeanu, P., Kuritzky, A., Korczyn, A. D. Familial levodopa-responsive parkinsonian-pyramidal syndrome Mov. Disord. 9: 673-675, 1994.
8. Shojaee, S., Sina, F., Banihosseini, S. S., Kazemi, M. H., Kalhor, R., Shahidi, G.-A., Fakhrai-Rad, H., Ronaghi, M., Elahi, E. Genome-wide linkage analysis of a parkinsonian-pyramidal syndrome pedigree by 500 K SNP arrays. Am. J. Hum. Genet. 82: 1375-1384, 2008.

Алгоритми за диагностициране на заболяването

Алгоритми за диагностициране на заболяването: Съгласно Национален консенсус за диагностика и лечение на Паркинсоновата болест.

Анамнезата: Ювенилна парализа ажитанс на Hunt е с начало в юношеството или по-рано на типичен паркинсонизъм с тремор, масковиден фациес, брадикинезия, дизартрия, ригидност и понякога дистония. Прогресията на синдрома е много бавна. PARK 15 започва във второ и началото на трето десетилетие с картина парализа ажитанс и пирамидни белези.

Диференциалната диагноза на заболяването: болест на Wilson; други форми на атипичен паркинсонизъм с ранно начало;

Лабораторни, образни и хистологични изследвания: Panagariya и колеги (2007) съобщава за SPECT промени при един пациент с хипоперфузия в ляв фронтопариетален регион и базални ганглии в ляво, както и минимална хипоперфузия на ляв темпорален лоб.

Генетични изследвания и медико-генетично консултиране: PARK15 още известен като паркинсон-пирамиден синдром се причинява от хомозиготна или комбинирана хетерозиготна мутация на FBXO7 гена на хромозома 22q12 с автозомно-рецесивно (АР) унаследяване.

В т.ч. научни публикации от последните пет години и приложена библиографска справка

1. Национален консенсус за диагностика и лечение на Паркинсоновата болест, Двигателни заболявания, 2013, 10, 1.
2. Hunt, J. R. Progressive atrophy of the globus pallidus (primary atrophy of the pallidal system): a system disease of the paralysis agitans type, characterized by atrophy of the motor cells of the corpus striatum; a contribution to the functions of the corpus striatum. Brain 40: 58-148, 1917
3. Allen, N., Knopp, W. Hereditary parkinsonism-dystonia with sustained control by L-

DOPA and anticholinergic medication. Adv. Neurol. 14: 201-213, 1976.
4. Martin, W. E., Resch, J. A., Baker, A. B. Juvenile parkinsonism. Arch. Neurol. 25: 494-500, 1971.
5. Davison, C. Pallido-pyramidal disease. J. Neuropath. Exp. Neurol. 13: 50-59, 1954.
6. Lange, E., Poppe, W. Klinischer Beitrag zum Krankheitsbild der progressiven Pallidumatrophie (van Bogaert). Psychiat. Neurol. (Basel) 146: 176-192, 1963.
7. Nisipeanu, P., Kuritzky, A., Korczyn, A. D. Familial levodopa-responsive parkinsonian-pyramidal syndrome Mov. Disord. 9: 673-675, 1994.
8. Panagariya, A., Sharma, B., Dev, A. Pallido-pyramidal syndrome: a rare entity. (Letter) Indian J. Med. Sci. 61: 156-157, 2007.
9. Shojaee, S., Sina, F., Banihosseini, S. S., Kazemi, M. H., Kalhor, R., Shahidi, G.-A., Fakhrai-Rad, H., Ronaghi, M., Elahi, E. Genome-wide linkage analysis of a parkinsonian-pyramidal syndrome pedigree by 500 K SNP arrays. Am. J. Hum. Genet. 82: 1375-1384, 2008.
10. Di Fonzo, A., Dekker, M. C. J., Montagna, P., Baruzzi, A., Yonova, E. H., Correia Guedes, L., Szczerbinska, A., Zhao, T., Dubbel-Hulsman, L. O. M., Wouters, C. H., de Graaff, E., Oyen, W. J. G., Simons, E. J., Breedveld, G. J., Oostra, B. A., Horstink, M. W., Bonifati, V. FBXO7 mutations cause autosomal recessive, early-onset parkinsonian-pyramidal syndrome. Neurology 72: 240-245, 2009.
11. Di Fonzo, A., Dekker, M. C. J., Montagna, P., Baruzzi, A., Yonova, E. H., Correia Guedes, L., Szczerbinska, A., Zhao, T., Dubbel-Hulsman, L. O. M., Wouters, C. H., de Graaff, E., Oyen, W. J. G., Simons, E. J., Breedveld, G. J., Oostra, B. A., Horstink, M. W., Bonifati, V. FBXO7 mutations cause autosomal recessive, early-onset parkinsonian-pyramidal syndrome. Neurology 72: 240-245, 2009

Алгоритми за лечение на заболяването

Алгоритми за лечение на заболяването: Съгласно Национален консенсус за диагностика и лечение на Паркинсоновата болест

Терапевтичните подходи към заболяването, в това число консервативни и оперативни, техните предимства, рискове и очаквана ефективност: Има съобщения за подобрение на пациентите с този синдром от лечение с Леводопа и антихолинестеразни медикаменти.

В т.ч. научни публикации от последните пет години и приложена библиографска справка

1. Национален консенсус за диагностика и лечение на Паркинсоновата болест, Двигателни заболявания, 2013, 10, 1.
2. Allen, N., Knopp, W. Hereditary parkinsonism-dystonia with sustained control by L-DOPA and anticholinergic medication. Adv. Neurol. 14: 201-213, 1976.
3. Martin, W. E., Resch, J. A., Baker, A. B. Juvenile parkinsonism. Arch. Neurol. 25: 494-500, 1971.
4. Horowitz, G., Greenberg, J. Pallido-pyramidal syndrome treated with levodopa. J. Neurol. Neurosurg. Psychiat. 38: 238-240, 1975.
5. Shojaee, S., Sina, F., Banihosseini, S. S., Kazemi, M. H., Kalhor, R., Shahidi, G.-A., Fakhrai-Rad, H., Ronaghi, M., Elahi, E. Genome-wide linkage analysis of a parkinsonian-pyramidal syndrome pedigree by 500 K SNP arrays. Am. J. Hum. Genet. 82: 1375-1384, 2008.
6. Di Fonzo, A., Dekker, M. C. J., Montagna, P., Baruzzi, A., Yonova, E. H., Correia Guedes, L., Szczerbinska, A., Zhao, T., Dubbel-Hulsman, L. O. M., Wouters, C. H.,

de Graaff, E., Oyen, W. J. G., Simons, E. J., Breedveld, G. J., Oostra, B. A., Horstink, M. W., Bonifati, V. FBXO7 mutations cause autosomal recessive, early-onset parkinsonian-pyramidal syndrome. Neurology 72: 240-245, 2009.
Алгоритми за проследяване на заболяването
Алгоритми за проследяване на заболяването (Необходимостта от последващи болнични и извънболнични грижи; Необходимостта от консултации с други специалисти): Съгласно Национален консенсус за диагностика и лечение на Паркинсоновата болест. Прогнозата на заболяването: Добра прогноза поради добрия отговор на Л-Допа терапията и без значимо влияние върху продължителността на живот.
В т.ч. научни публикации от последните пет години и приложена библиографска справка
1. Национален консенсус за диагностика и лечение на Паркинсоновата болест, Двигателни заболявания, 2013, 10, 1. 2. Allen, N., Knopp, W. Hereditary parkinsonism-dystonia with sustained control by L-DOPA and anticholinergic medication. Adv. Neurol. 14: 201-213, 1976. 3. Martin, W. E., Resch, J. A., Baker, A. B. Juvenile parkinsonism. Arch. Neurol. 25: 494-500, 1971. 4. Horowitz, G., Greenberg, J. Pallido-pyramidal syndrome treated with levodopa. J. Neurol. Neurosurg. Psychiat. 38: 238-240, 1975. 5. Shojaee, S., Sina, F., Banihosseini, S. S., Kazemi, M. H., Kalhor, R., Shahidi, G.-A., Fakhrai-Rad, H., Ronaghi, M., Elahi, E. Genome-wide linkage analysis of a parkinsonian-pyramidal syndrome pedigree by 500 K SNP arrays. Am. J. Hum. Genet. 82: 1375-1384, 2008. 6. Di Fonzo, A., Dekker, M. C. J., Montagna, P., Baruzzi, A., Yonova, E. H., Correia Guedes, L., Szczerbinska, A., Zhao, T., Dubbel-Hulsman, L. O. M., Wouters, C. H., de Graaff, E., Oyen, W. J. G., Simons, E. J., Breedveld, G. J., Oostra, B. A., Horstink, M. W., Bonifati, V. FBXO7 mutations cause autosomal recessive, early-onset parkinsonian-pyramidal syndrome. Neurology 72: 240-245, 2009.
Алгоритми за рехабилитация на заболяването
Алгоритми за рехабилитация на заболяването: Съгласно Национален консенсус за диагностика и лечение на Паркинсоновата болест.
В т.ч. научни публикации от последните пет години и приложена библиографска справка
1. Национален консенсус за диагностика и лечение на Паркинсоновата болест, Двигателни заболявания, 2013, 10, 1.
Необходими дейности за профилактика на заболяването (ако такива са приложими)
Дейности за профилактика на заболяването: Първична, вторична и третична превенция: PARK15 още известен като паркинсон-пирамиден синдром се причинява от хомозиготна или комбинирана хетерозиготна мутация на FBXO7 гена на хромозома 22q12 с автозомно-рецесивно (AP) унаследяване. Това би могло да предостави възможност за пренатална диагностика и консултация.
В т.ч. научни публикации от последните пет години и приложена библиографска справка
1. Shojaee, S., Sina, F., Banihosseini, S. S., Kazemi, M. H., Kalhor, R., Shahidi, G.-A.,

Fakhrai-Rad, H., Ronaghi, M., Elahi, E. Genome-wide linkage analysis of a parkinsonian-pyramidal syndrome pedigree by 500 K SNP arrays. Am. J. Hum. Genet. 82: 1375-1384, 2008.
2. Di Fonzo, A., Dekker, M. C. J., Montagna, P., Baruzzi, A., Yonova, E. H., Correia Guedes, L., Szczerbinska, A., Zhao, T., Dubbel-Hulsman, L. O. M., Wouters, C. H., de Graaff, E., Oyen, W. J. G., Simons, E. J., Breedveld, G. J., Oostra, B. A., Horstink, M. W., Bonifati, V. FBXO7 mutations cause autosomal recessive, early-onset parkinsonian-pyramidal syndrome. Neurology 72: 240-245, 2009

Предложения за организация на медицинското обслужване на пациентите и за финансиране на съответните дейности, съобразени с действащата в страната нормативна уредба

Създаването на Национален експертен център „Редки невродегенеративни заболявания, протичащи с когнитивни, поведенчески и моторни нарушения" за диагностика, лечение и проследяване и рехабилитация включително и на пациенти с това заболявания под ръководството на чл.кор.проф.д-р Л. Трайков, дмн (национален експерт с най-голям опит и принос за диагностиката и лечението на тези заболявания).

Описание на опита с конкретни пациенти със съответното рядко заболяване (ако има такъв)

Опитът на кандидатстващия експертен център под ръководството на чл. кор. проф.Трайков за диагноза и лечение на редки заболявания, протичащи с паркинсонизъм с и без когнитивни нарушения, датира от 2001 година със създаването на център за диагноза и лечение на невродегенеративни заболявания, протичащи с деменция и допълнително на център за диагноза и лечение на Паркинсонова болест. От дълги години този център е реферирaн център за заболявания, протичащи с паркинсонизъм с и без когнитивни нарушения, особено за комплексни, редки и наследствени случаи. През годините вследствие на натрупания опит и труд, както и значителен брой на пациенти с тези редки заболявания, реферирани към центъра са осъществени няколко дисертации в областта: 1. Когнитивни нарушения при Паркинсонова болест (защитена дисертация за доктор по медицина от д-р Мария Петрова, 2010 г., ръководител: чл.-кор. проф. Лъчезар Трайков), 2. Лонгитудинално проследяване на когнитивните нарушения при Паркинсонова болест (защитена дисертация за доктор по медицина от д-р Явор Желев, 2012 г., ръководител: чл.-кор. проф. Лъчезар Трайков) и 3. Клинико-генетични корелации при невродегенеративни заболявания, протичащи с паркинсонизъм (защитена дисертация за доктор по медицина от д-р Радка Павлова, 2013 г., ръководител: чл.-кор. проф. Лъчезар Трайков). Събрана е база данни за отделни пациенти с отделни групи редки заболявания, протичащи с паркинсонизъм с и без когнитивен дефицит с подробно фенотипизиране на всеки един случай, което дава възможност за добър мониторинг на пациентите, както и изследователски анализ върху характеристиката на отделните заболявания. Дейността на центъра по отношение на диагноза и лечение на редки заболявания, протичащи с моторни и когнитивни нарушения, обхваща всички диагностични дейности съобразно новите диагностични критерии на тези заболявания, включително допълнителни изследвания, които са нужни за диференциална диагноза на атипични/ранни/наследствени случаи, включващи изследвания за биомаркери, невроизобразяващи и генетични фактори.

Публикации:

1. Pavlova R, Mehrabian S, Petrova M, Skelina S, Mihova K, Jordanova A, Mitev V, Traykov L. Cognitive, neuropsychiatric, and motor features associated with apolipoprotein E ε4 allele in a sample of Bulgarian patients with late-onset Parkinson's disease. Am J Alzheimers Dis Other Demen. 2014 Nov;29(7):614-9.
2. Petrova M, Raycheva M, Traykov L. Cognitive profile of the earliest stage of dementia in Parkinson's disease. Am J Alzheimers Dis Other Demen. 2012 Dec;27(8):614-9.
3. Petrova M, Raycheva M, Zhelev Y, Traykov L. Executive functions deficit in Parkinson's disease with amnestic mild cognitive impairment. Am J Alzheimers Dis Other Demen. 2010 Aug;25(5):455-60.
4. Kochev D, Petrova J, Petrova M, Krastev D, Traykov L. Possibility of combined assessment of biomarkers in early Parkinson's disease. International Journal of Science and Research, 2014, 3, 10, 1332-1334;
5. Петрова М., Райчева М., Пенев Л., Григорова О., Желев Я., Трайков Л. Когнитивни различия между леко когнитивно нарушение и деменция при Паркинсонова болест. Българска Неврология, 2010, 4, 168-172.
6. Петрова М., Райчева М., Мехрабиан Ш., Желев Я., Ангов Г. Трайков Л. Връзки между депресията и когнитивните дефицити при пациенти с Паркинсонова болест и леко когнитивно нарушение. Българска Неврология, 2010, 10, 3, 122-125.
7. Петрова М., Трайков Л. Рискови фактори за развитие на когнитивни нарушения и деменция при Паркинсонова болест. Българска Неврология, 2010, 10, 3, 98-102.
8. Петрова М., Райчева М., Трайков Л. Връзки между предоминантния моторен подтип и когнитивни дефицити при пациенти с Паркинсонова болест с леко когнитивно нарушения. Българска Неврология, 2010, 4, 161-164.
9. Петрова М., Трайков Л. Особености в профила и диагностика на когнитивните нарушения при Паркинсонова болест, Неврология и Психиатрия, 2011, 1, 43.
10. Павлова Р, Мехрабиан Ш, Скелина С, Желев Я, Михова К, Кънева Р, Митев В, Йорданова А, Трайков Л. Характеристика на дегенеративния паркинсонов синдром в зависимост от Аполипопротеин Е генотипа. Неврология и психиатрия, 4, 30-33, 2014;
11. Петрова М., Григорова О, Желев Я., Павлова Р., Владимиров Б., Трайков Л. Влияние на Дуодопа върху моторните и немоторите усложнения при напреднала Паркинсонова болест. МЕДИКАРТ: Неврология и Психиатрия, 2014, 1, 24-29.
12. Кочев Д., Петрова Ю., Петрова М., Трайков Л. Оценка на ехогенността на субстанция нигра при пациенти с ранна Паркинсонова болест. Медицински Преглед, 2014, 50, 5, 45-47.
13. R. Pavlova, K. Mihova, S. Mehrabian, M. Petrova, S. Skelina, R. Kaneva, V. Mitev, L. Traykov. Novel LRRK2 6165C>G mutation in a patient with Parkinson's disease-dementia: a case report. In: JOINT CONGRESS OF EUROPEAN NEUROLOGY Istanbul, Turkey, May 31-June 3, 2014.

14. Pavlova R., K. Mihova, S. Mehrabian, M. Petrova, S. Skelina, R. Kaneva, A. Jordanova, V. Mitev, L. TraykovLRRK2 mutation c.4536+3A>G in a patient with multiple system atrophy: a case report. In: In: JOINT CONGRESS OF EUROPEAN NEUROLOGY Istanbul, Turkey, May 31-June 3, 2014.

Genome-wide Linkage Analysis of a Parkinsonian-Pyramidal Syndrome Pedigree by 500 K SNP Arrays

Seyedmehdi Shojaee,[1] Farzad Sina,[4] Setareh Sadat Banihosseini,[5] Mohammad Hossein Kazemi,[5] Reza Kalhor,[6] Gholam-Ali Shahidi,[4] Hossein Fakhrai-Rad,[7] Mostafa Ronaghi,[7] and Elahe Elahi[2,3,*]

Robust SNP genotyping technologies and data analysis programs have encouraged researchers in recent years to use SNPs for linkage studies. Platforms used to date have been 10 K chip arrays, but the possible value of interrogating SNPs at higher densities has been considered. Here, we present a genome-wide linkage analysis by means of a 500 K SNP platform. The analysis was done on a large pedigree affected with Parkinsonian-pyramidal syndrome (PPS), and the results showed linkage to chromosome 22. Sequencing of candidate genes revealed a disease-associated homozygous variation (R378G) in *FBXO7*. *FBXO7* codes for a member of the F-box family of proteins, all of which may have a role in the ubiquitin-proteosome protein-degradation pathway. This pathway has been implicated in various neurodegenerative diseases, and identification of *FBXO7* as the causative gene of PPS is expected to shed new light on its role. The performance of the array was assessed and systematic analysis of effects of SNP density reduction was performed with the real experimental data. Our results suggest that linkage in our pedigree may have been missed had we used chips containing less than 100,000 SNPs across the genome.

Genome-wide linkage analyses of Mendelian diseases have traditionally been done with microsatellite markers.[1,2] The potential value of using single-nucleotide polymorphisms (SNPs) in such analysis has been more recently proposed.[3–7] Their advantages largely stem from their higher density and global distribution in the human genome. Robust SNP genotyping technologies and data analysis programs have encouraged researches to use SNP platforms in linkage studies.[8–12] Platforms used to date have been 10 K chip arrays; however, the possible value of interrogating SNPs at a higher density in linkage analysis has been considered.[11,13] Here, we present what is to the best of our knowledge the first genome-wide linkage analysis with a 500 K SNP platform. The analysis was performed on a large Iranian pedigree affected with Parkinsonian-pyramidal syndrome (PPS [MIM 260300]; Figure 1). It resulted in the identification of *FBXO7* as the likely disease-causing gene. The performance of the array was assessed and systematic analysis of effects of SNP density reduction on information content, maximum LOD scores, and length of linked area was performed. We surmised that for our particular pedigree structure, linkage may well have been missed had we used chips containing less than 100,000 SNPs.

PPS is a hypokinetic rigid disorder, the most common example of which is Parkinson's disease.[14] PPS is a rare disorder that exhibits both Parkinsonian and pyramidal-associated symptoms. Approximately 20 patients have been reported in the literature.[14–17] Symptoms, which may be vague in the beginning, start in young adulthood, progress relatively slowly, and may culminate in severe movement incapacity. Response to levadopa is usually dramatic and sustained for many years. Most, but not all, reported cases have been familial and associated with parental consanguinity, suggesting autosomal-recessive inheritance.[14,16,18]

The research was performed in accordance with the Helsinki Declaration and with approval of the ethics boards of the University of Tehran. All participants consented to participate after being informed of the nature of the research. Living members of the PPS pedigree were examined by two movement-disorder specialists, and many were also examined by specialists in other fields. Ten individuals dispersed in two generations were assessed to be affected with PPS (Figure 1). An 11th individual (5043) was assessed as having been affected based on phenotypic features reported by family members. All other living members of the pedigree were assessed to be normal.

Clinical information on the ten affected individuals is presented in Table 1. All affecteds exhibited equinovarus deformity since childhood, which is usually indicative of a genetic central nervous system disorder.[19] None had symptoms associated with cerebellar malfunction. All exhibited Babinski signs, spasticity, and hyperactive DTR. The Babinski signs in all were initially unilateral, and later became bilateral. Spasticity was restricted to lower limbs in most patients. Onset of pyramidal symptoms in the patients was always in the third decade of life. At the time of writing, detectable extrapyramidal symptoms have evolved only in the three most severely affected individuals (5001, 5003, and 5027). These symptoms became evident 5 to 20 years after appearance of pyramidal

[1]Department of Biotechnology, [2]School of Biology, [3]Center of Excellence in Biomathematics, School of Mathematics, Statistics and Computer Science, College of Science, University of Tehran, Tehran, Iran; [4]Iran University of Medical Sciences, Hazrat Rasool Hospital, Tehran, Iran; [5]Tehran University of Medical Sciences, Tehran, Iran; [6]Molecular and Computational Biology, Department of Biological Sciences, University of Southern California, Los Angeles, CA 90089, USA; [7]Stanford Genome Technology Center, Stanford University, Palo Alto, CA 94304, USA
*Correspondence: elaheelahi@ut.act.ir, elahe.elahi@gmail.com
DOI 10.1016/j.ajhg.2008.05.005.

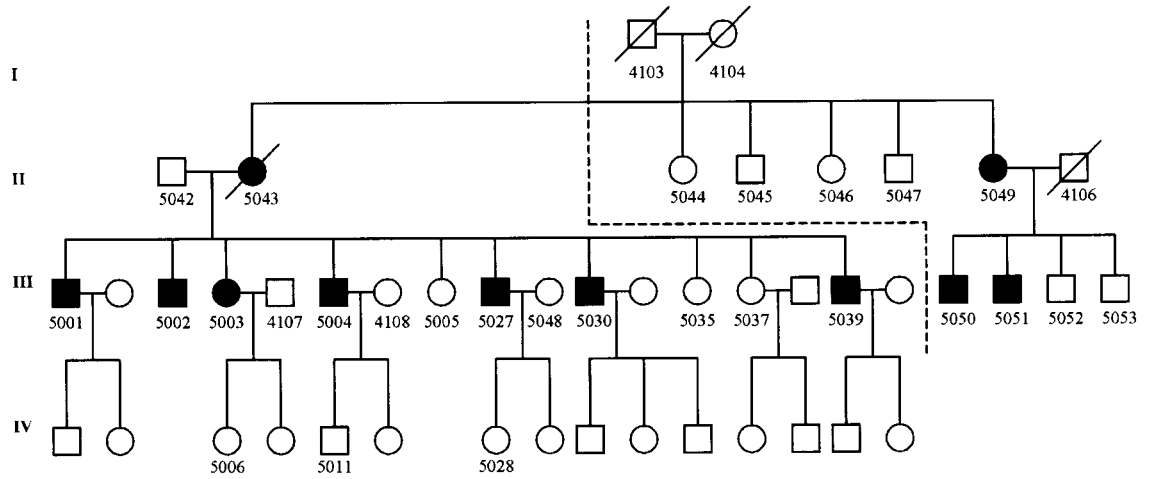

Figure 1. Parkinsonian-Pyramidal Syndrome Pedigree
Affected individuals are shown by shading. All individuals with number ID were included in pedigree file imported into MERLIN. Only living individuals whose ID numbers start with 5 were genotyped on the chips. Individuals 5042 and 5043 and individuals 5049 and 4106 were each reported to be distally related, but consanguinity between the individuals is not indicated because the exact relationship between the individuals could not be ascertained. The dashed line delineates the margin between the two minimized pedigrees.

symptoms. The extrapyramidal symptoms of patient 5027 were rapidly alleviated by L-dopa, and the response has been sustained for 4 years. Patients 5001 and 5003 were not cooperative in receiving treatment. None of the patients exhibited tremor, upgaze paresis, Myerson's sign, or dementia. Brain and spinal MRI, EEG, ocular examination, and EMG were performed on individuals 5001, 5027, and 5030; the results were normal. A complete laboratory metabolic workup on these patients, which included measurement of serum ceruloplasmin and copper level, did not show any biochemical abnormality. Movement anomalies and some other features of affected individuals are evident in video recordings and photograph (see Movies S1–S4 and Figure S1 available online). Reasons by which diseases other than Parkinsonian-pyramidal syndrome were excluded are given in Table S2.

Genomic DNA was prepared from venous blood of 10 affected and 14 unaffected members of the pedigree. Genome-wide linkage scan was performed on these DNAs with the GeneChip Human Mapping 500K Array Set according to the manufacturer's recommended protocol (Affymetrix, Santa Clara, CA). Arrays were processed through Affymetrix microfluidics stations, and images were obtained with an Affymetrix Gene Array scanner. Raw microarray feature intensities were processed with GeneChip Genotyping Analysis Software v.4.1.0.26 (GTYPE) to derive SNP genotypes. GTYPE uses the Bayesian Robust Linear Model with Mahalanobis distance classifier (BRLMM) algorithm for genotype calling.

SNP call rate with BRLMM for the 24 individuals tested ranged from 98.12% to 99.62% and was 99.15% on the average. Across all genotype calls of all individuals, 26% (range 25%–27%) were heterozygous. Concordance of the genotypes of the 50 SNPs shared on the two arrays of the 24 individuals genotyped was 99.76%. On the average, 0.58% of 10,524 X chromosome SNPs were genotyped as

Table 1. Clinical Features of Affected Individuals

	Extrapyramidal Symptoms				Pyramidal Symptoms				
	Rigidity	Bradykinesia	Hypomimia	Monotone Speech	Babinski Signs	Spasticity	Hyperactive DTR	Scissor Gait	Equinovarus Deformity
5001*	+	+	+	+	+	+	+	unable to walk	+
5002	-	-	-	-	+	+	+	-	+
5003*	+	+	+	unable to speak	+	+	+	unable to walk	+
5004	-	-	-	-	+	+	+	-	+
5027*	+	+	+	+	+	+	+	+	+
5030	-	-	-	-	+	+	+	-	+
5039	-	-	-	-	+	+	+	-	+
5049	-	-	-	-	+	+	+	-	+
5050	-	-	-	-	+	+	+	-	+
5051	-	-	-	-	+	+	+	-	+

*The most severely affected individuals.

heterozygous in each of the 14 male individuals genotyped. Often, the same SNP was miscalled in several male individuals. Genotypic information was obtained for the mother (5049) of only four of these male individuals, and these four were siblings. Approximately 7000 homozygous X chromosome SNPs were observed in this female individual, and alternate allele genotype calls for these SNPs in her sons allows for detection of another set of miscalls. It was estimated that 0.1% of these SNPs were miscalled per individual in this part of the pedigree. By extrapolation, the transmission error rate per generation for the entire data set is expected to be approximately 0.7%. In fact, GTYPE detected Mendelian errors in 0.06% of the SNPs dispersed throughout the genome per individual genotyped. By comparison with the more telling SNPs of the X chromosome, the figures suggest that only about 10% of the miscalls on the autosomal chromosomes are detected. GTYPE removed SNPs that were detected as Mendelian errors. It subsequently removed 42% of the remaining SNPs because only one allele for each was observed in our entire pedigree, or because of a call rate less than 90% among all the individuals. The number of remaining SNPs was 286,508.

For genetic analysis, an appropriate GTYPE option was used to automatically export by chromosome genotype calls into MERLIN.[20] Because of the large size of the pedigree, it was split into two smaller pedigrees for analysis (Figure 1). Individuals 5042 and 5043 were defined as the ancestors of one of the minimized pedigrees, and individuals 4103 and 4104 as the ancestors of the other. Individual 5043 was included only in the first minimized pedigree. The PedWipe option in MERLIN assessed 0.3% (based on chromosome 22 data) of the calls unlikely to be correct and removed these. MERLIN was then used to assess information content of the arrays and to perform multipoint nonparametric (NPL) and parametric linkage analysis. Inheritance of PPS in affected kindreds has been proposed to be autosomal recessive, but sporadic cases have also been reported and the possibility that this condition may be heterogeneous has been suggested.[14–16] The rarity of the condition, the inbreeding reported in our pedigree (especially in generations I, II, and before), and the absence of disease among individuals of generation IV are strongly suggestive of an autosomal-recessive mode of inheritance in this pedigree. On the other hand, the possibility that onset of symptoms had not yet manifested in some young generation IV individuals, ambiguity of consanguinity between parents of affected individuals, and the observation of disease in consecutive generations made it unwise to rule out possible dominant inheritance.

Merlin calculated a nonparametric logarithm of odds (LOD) score by use of the Kong and Cox exponential model.[21] MERLIN also generated parametric LOD scores under assumption of disease allele frequency of 0.0001 and full penetrance. Because of limitations of computer memory, data of three unaffected individuals in generation IV (individuals 5006, 5011, and 5028) and the unaffected mother of one of these (individual 5048) were not included in the original analysis. The information content and results of scans for all the chromosomes under the NPL, autosomal-recessive, and autosomal-dominant models based on data of 20 individuals are shown in Figures S2–S5. After having focused on chromosome 22, data on all 24 individuals were included for the analysis of this relatively small chromosome. The average information content for each of the 23 chromosomes was notable and ranged from 0.948 to 0.996. Maximum potential LOD score calculated for our pedigree structure by MERLIN under NPL was 4.21 ($Z = 9.806$; $p = 10^{-5}$).[20] NPL analysis resulted in LOD scores of greater-than-suggestive LOD score 2.1 ($p < 0.001$) on chromosomes 3, 5, 7, 11, 14, 15, and 22, and LOD scores greater-than-significant LOD score of 3.3 ($p < 0.00005$) on chromosomes 5, 11, 14, and 22.[22] Because the peaks of chromosomes 5, 11, and 14 each included at most 6 SNPs and covered a maximal range of 0.2 cM, it was assumed they were probably due to erroneous genotypings not detected by the various error-checking protocols. On chromosome 22, a broad region extending from 4.17 to 28.18 cM was associated with an average LOD score of 2.90, and another region extending from 34.40 to 41.93 cM (28,934,667 bp–34,951,655 bp) was associated with an average LOD score of 4.08 (average $p = 0.00003$) (Figure 2A). Within the latter region, the maximum predicted LOD score of 4.21 was observed in region extending from 36.58 to 39.98 cM. Parametric analysis under an autosomal-dominant model resulted in only negative LOD scores on all chromosomes except 22, on which an average score of 0.81 was achieved at region extending from 34.40 to 35.97 cM (maximum LOD = 1.57 at 34.57 cM) (Figure 2A). Finally, analysis under an autosomal-recessive model resulted in positive LOD scores on chromosomes 5 (average LOD of peak = 3.00), 15 (average LOD = 1.18), and 22. The region on chromosome 22 was broad and extended from 30.48 to 56.24 cM; the average associated LOD score was 2.825 (Figure 2A). Within this region, there was a peak extending from 34.50 cM to 36.88 cM (29,055,302 bp–31,414,345 bp), with an average associated LOD score of 3.32. The maximum score achieved within the region was 3.39. The peak region on chromosome 22 as compared to the peak region of chromosome 5 was considered a better candidate region because a significantly overlapping region of chromosome 5 was not observed under the NPL model. Furthermore, it was observed that the genotypes of the affected individuals for many of the SNPs in the chromosome 5 region were heterozygous. For example, at the SNP position associated with the maximum LOD score (3.38), seven of the ten affected individuals genotyped were heterozygous. Twenty simulations for each of the inheritance models by means of the chromosome 22 genotypes resulted in maximum LOD scores of 1.54, −5.87, and −1.08, respectively, for the NPL, autosomal-dominant, and autosomal-recessive models (not shown). The information content across the length of chromosome 22 approached 1, and the average was 0.964 (Figure 2B).

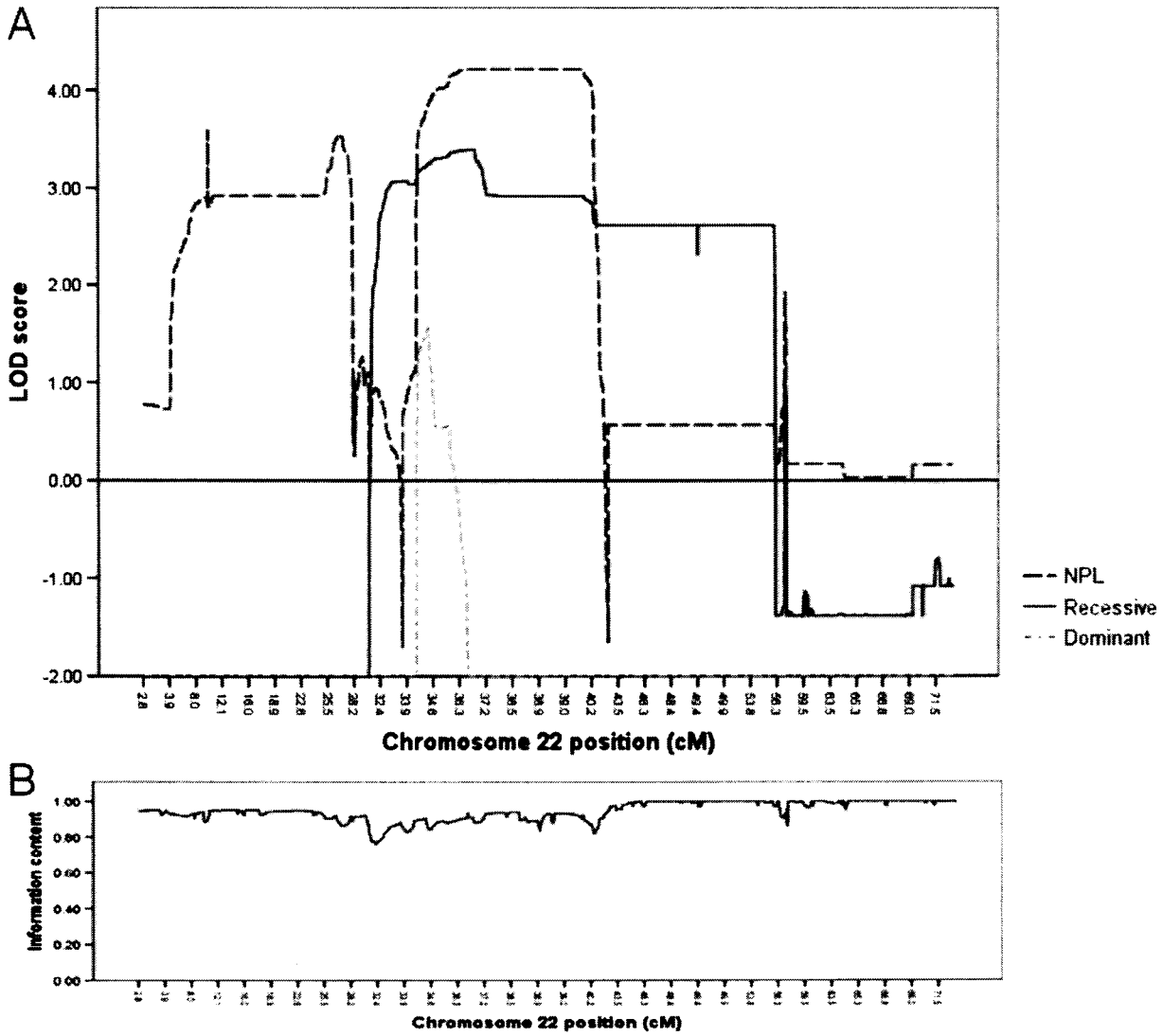

Figure 2. LOD Plots and Information Content for Chromosome 22
(A) The LOD plots under NPL, autosomal-dominant, and autosomal-recessive models of disease inheritance are shown.
(B) Information content for chromosome 22.

Visual inspection, in fact, showed that all affected individuals and only affected individuals shared a homozygous genotype for all 209 SNPs within the region (2.38 cM) having the average LOD value of 3.32. It was surmised that the locus most likely associated with the disease status was on chromosome 22 and that its mode of inheritance in the pedigree was autosomal recessive. Interestingly, results of haplotyping of chromosome 22 by MERLIN revealed that one of the recombination events that delimited the linked region occurred in five meioses. This event occurred between rs134176 and rs738996, suggesting a recombination hotspot. Reanalysis of chromosome 22 data by means of clusters at r^2 values of 0.4 produced NPL, autosomal-dominant, and autosomal-recessive LOD plots nearly identical to those produced without clustering (not shown).

Annotations provided by GTYPE and the NCBI database were used to identify genes within chromosomal regions that showed linkage. The critical region of 34.50–36.88 cM on chromosome 22 contains 34 annotated genes. To prioritize the region to be examined, we reasoned that the region containing the causative gene should cause a drop in LOD score under the dominant model, because at least nine unaffected individuals were expected to carry one copy of the disease-causing allele. Furthermore, we expected the disease-causing gene to be included in the region associated with a high LOD score under the NPL model. The right border of the linked region under the dominant model was at 35.97 cM, and the overlap between the critical region under the recessive model and the region having an average LOD score of 4.08 under

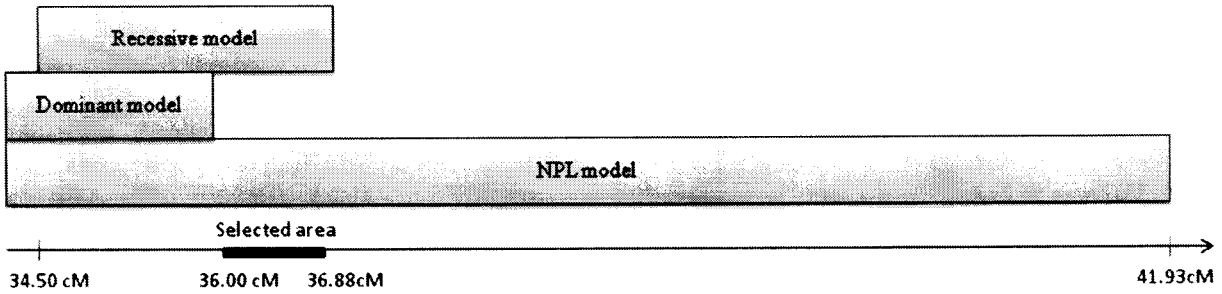

Figure 3. Prioritization of Linkage to Region of 0.9 cM on Chromosome 22
Regions on chromosome 22 showing maximum linkage to disease phenotype under NPL (34.40–41.93 cM), autosomal-dominant (34.40–35.97 cM), and autosomal-recessive (34.49–36.88 cM) models are shown as overlapping regions. The solid gray bar (36.00–36.88 cM) indicates region prioritized for selection of candidate genes.

the NPL model extended from 36.00 cM to 36.88 cM (Figure 3). Four genes are annotated in this region of chromosome 22: ret finger protein-like 3 (*RFPL3*), C22orf28 (alias *HSPC117*), bactericidal/permeability-increasing protein-like 2 (*BPIL2*), and F-box protein 7 (*FBXO7*). Part of synapsin III (*SYN3*) also lies within the region, and TIMP metallopeptidase inhibitor 3 (*TIMP3*) lies just downstream. C22orf28, *FBXO7* (MIM 605648), SYN3 (MIM 602705), and *TIMP3* (MIM 188826) were considered to be good biological candidate genes for the disease phenotype of our pedigree.[23–28]

The exons and flanking intronic sequences of these four genes were amplified from the DNA of patient 5001 by PCR and subsequently sequenced with the ABI Big Dye terminator chemistry and an ABI Prism 3700 instrument (Applied Biosystems, Foster City, CA). Sequences were analyzed with the Sequencher software (Gene Codes Corporation, Ann Arbor, MI) (Table S1). The frequencies of alleles at variant positions in different populations were obtained from the HapMap site when available. Predicted effects of variant sequences on splicing were determined by comparison with known canonical splice site motifs by means of NNsplice 0.9 and genescan. For determination of extent of conservation of amino acids altered due to nucleotide variations found, the amino acid sequences of homologous proteins from other species were obtained from NCBI and aligned with the ClustalW 1.83 software.

Five sequence variations in the homozygous state were observed in C22orf28, six in *FBXO7*, three in *SYN3*, and none in TIMP3 (Table 2). Except for g.18550C→G in *FBXO7*, the observed variations were considered not to be associated with disease status. They were assessed not to affect splicing, and most were also reported at relatively high frequencies in other populations (0.1–0.9).

FBXO7 codes two cDNA and protein isoforms. The isoform 1 protein is longer than the isoform 2, but amino acid 92 to amino acid 522 of the former correspond exactly to amino acids 7 to 443 of the latter. Because references to *FBXO7* in the literature are generally with respect to isoform 1 of the cDNA and protein, we will henceforth make references with respect to this isoform.[29–31] The c.1132C→G change results in the nonconservative amino acid substitution of glycine for arginine at position 378 (R378G) in the F-box protein 7. Arginine at position 378 is completely conserved in all F-box protein 7 proteins sequenced, including the protein in species as distally related as humans and the purple sea urchin (Table S3). Furthermore, it lies within a well-conserved region of the protein and within a completely conserved -RDF- motif. By sequencing, the variant allele was also observed in the homozygous state in three other affected individuals (5003, 5049, and 5051) and in the heterozygous state in one unaffected obligate carrier (5005). By an ARMS-PCR target mutation analysis assay, it was shown that the remaining six available affected pedigree members each carried two mutant alleles and that eight obligate carriers each carried one mutant allele. These data showed segregation of R367G with the disease phenotype in an autosomal-recessive pattern in the pedigree. The mutant allele was not observed in the chromosomes of 800 control individuals. 600 of the controls were unrelated healthy Iranian individuals over the age of 60 without self-reported movement or neurological disorders, and 200 were unrelated Iranians diagnosed with Parkinson's disease.

Our results suggest that the mutation causing the R378G substitution in the FBXO7 protein is the cause of the disease phenotype exhibiting pyramidal and extrapyramidal anomalies in our pedigree. The condition was inherited in an autosomal-recessive fashion. *FBXO7* codes for a member of the F-box family of proteins. F-box proteins all contain an F-box motif, a motif consisting of ~40 amino acids that is functionally defined as one that can interact with the Skp1 component of the SCF (Skp1, Cdc53/Cullin1, F-box) protein complex.[30,32–34] FBXO7 also contains a proline-rich region (PRR) that is responsible for binding discs, large homolog 7 (*DLG7*, alias *HURP*), a known substrate of FBXO7.[30] The R378G mutation lies at or near the right border of the F-box motif and approximately 45 amino acids upstream of the left border of the PRR motif and may disrupt the function of either or both of these (Figure 4). Interactions of FBXO7 with proteins other than *DLG7* have also been reported and it has been suggested

Table 2. Sequence Variations

Gene	Gene Location[a]	cDNA Location[b]	Effect on Protein[c]	rs Number[d]	Allele Frequency Range[d,e]
C22orf28	g.3571A→G	c.172+77A→G	-	rs2076044	0.15–0.53
	g.3580C→T	c.172+86C→T	-	rs2076043	0.67–0.90
	g.3923C→T	c.173-84C→T	-	rs5754073	0.67–0.90
	g.17233T→G	c.1179+10T→G	-	rs2072818	0.48–0.79
	g.20160A→T	c.1410+151T→G	-	rs5994562	0.09–0.54
FBXO7	g.677T→G	c.122+272T→G [1] c.35T→G [2]	p.L12R [2]	rs8137714	-
	g.736C→A	c.122+331C→A [1] c.37+57C→A [2]	-	rs8140067	0.1–22
	g.4484G→A	c.343G→A [1] c.233G→A [2]	p.M115I [1] p.M36I [2]	rs11107	0.36–0.68
	g.16292T→C	c.872-75T→C[1] c.635-75T→C[2]	-	rs738982	0.36–0.68
	g.16444C→T	c.949C→T [1] c.712C→T [2]	p.L317L [1] p.L238L [2]	rs9726	0.36–0.68
	g.18550C→G	**c.1132C→G [1]** **c.895C→G [2]**	**p.R378G [1]** **p.R299G [2]**	ss99938574	**NA**
SYN3	g.75518C→A	c.461+209C→A [IIIa, IIIc]	-	rs183588	0–0.12
	g.477951G→C	c.1230+128G→C [IIIa, IIIc]	-	rs135123	0.1–0.19
	g.493006C→T	c.*1C→T [IIIa]	-	ss99938576	NA
		c.*118C→T [IIIc]	-		

Putative disease-associated variation is shown in bold. NA, not available.

[a] Gene positions in C22orf28, *FBXO7*, and *SYN3* are, respectively, with reference to sequences NT_011520.11 (nucleotides 12198804-12174138), NT_011520.11 (nucleotides 12261276-12285387), and NT_011520.11 (nucleotides 12793252-12299109).

[b] cDNA positions in C22orf28 are with reference to sequence NM_014306.3. cDNA positions in *FBXO7* are with reference to sequence NM_012179.3 for isoform 1 and and sequence NM_001033024.1 for isoform 2. cDNA positions in *SYN3* are with reference to sequence NM_003490.2 for isoform IIIa and sequence NM_133633.1 for isoform IIIc.

[c] Protein positions in F-box only protein 7 are with reference to sequence NP_036311.3 for isoform 1 and sequence NP_001028196.1 for isoform 2. Superscripts of cDNA and amino acid variations refer to respective isoforms.

[d] NCBI Build 36.2 was used to obtain all reference sequences.

[e] Range of frequency of the varied alleles observed in pedigree reported for populations of HapMap project. No sequence variations were observed in sequenced regions of gene *TIMP3*.

that some of the effects of FBXO7 are not mediated by ubiquitin-mediated degradation of the proteins with which it interacts.[35] And, of course, ubiquinitation may affect cellular functions other than proteolysis.[36,37]

The role of FBXO7 in neurons is not known. However, mutations affecting proteins involved in the ubiquitin-proteolytic pathway have been associated with various neurodegenerative diseases, including Parkinson's and Alzheimer's diseases, signifying the importance of this pathway in neuron function.[24] Mutations in *FBXO7* have not been observed in any of the aforementioned diseases. Functional studies need to be performed to confirm and expand on the genetic findings reported here.

The analysis performed on our pedigree produced data that allowed evaluation of the performance of the Affymetrix 500 K chips for linkage analysis. Although GTYPE seems to detect only a small fraction of the SNP miscalls, the number of miscalls in our analysis was sufficiently low not to preclude detection of linkage in our pedigree. As reported by others, the PedWipe option in MERLIN was very effective in removing faulty peaks caused by one or few SNPs (not shown). Consideration of effect of linkage disequilibrium (LD) on LOD scores is an issue when high-density marker platforms are used. However, this consideration is most important in sib pair analysis and multipedigree analysis, especially when parental

Figure 4. Schematic View of F-Box Only Protein 7, Isoform 1
Numbers on top indicate amino acid residue positions of left and right borders of F-box and proline-rich regions. The position of putative disease associated variation is shown below.

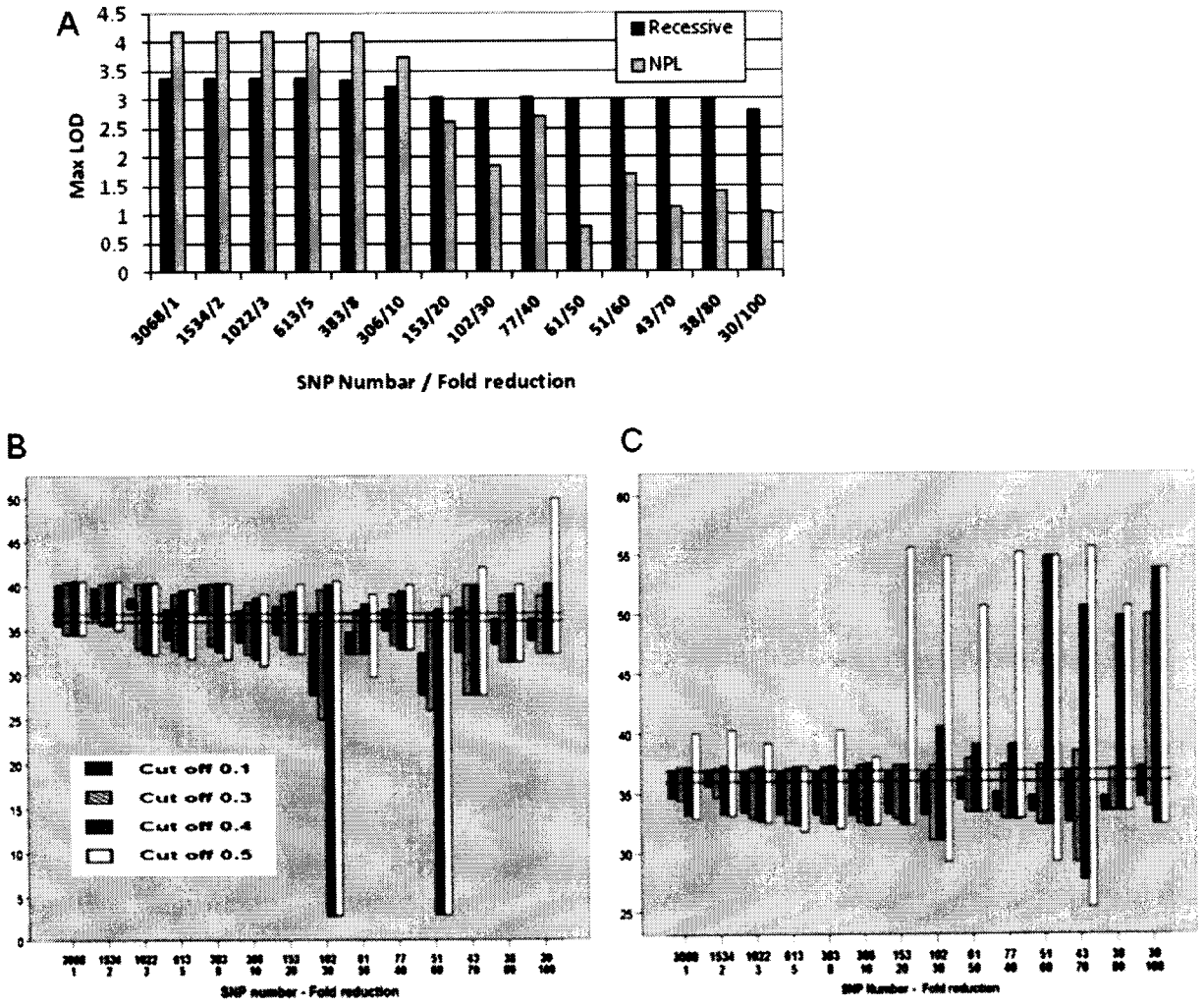

Figure 5. Effects of Reduction of Chromosome 22 SNP Numbers

(A) Effect on maximum LOD scores under NPL and recessive models of inheritance.

(B and C) Effect on position and length of linked area with cut offs of 0.1, 0.3, 0.4, and 0.5 below maximum LOD scores under NPL (B) and recessive (C) models.

The y axis shows cM along chromosome 22. The horizontal grid shows the 36.00–36.88 cM region.

genotypes are not available.[4,38–41] The effect is least important in linkage analysis by means of a single pedigree, as is the case in the present study. MERLIN allows for consideration of linkage disequilibrium by use of the Cluster option. Clustering effectively identifies adjacent markers that are in LD as a single marker and thus minimizes any possible effect LD may have on parameter being queried, i.e., LOD score. As expected, clustering had minimal effects on the LOD plots of our analysis.

Having identified the putative disease-causing gene, we attempted to ascertain the value of using a dense SNP map in our analysis under NPL and recessive models by systematically reducing the number of SNPs (Figures 5 and 6). A program was written in PERL for SNP reduction that allowed SNP selections starting at designated SNP and multiplier. The multiplier determines the number of SNPs to be removed between consecutive SNPs to be kept. Linkage analysis was repeated only for chromosome 22 SNPs while reducing the number of SNPs by factors ranging between 2 and 100. The average information content was reduced notably (Figure S6) and became uneven (not shown) across the length of chromosome 22 at greater than 20-fold reductions. In both models, the maximum LOD score progressively decreased with reduction in density of SNPs, but the effect was more pronounced in the NPL model (Figure 5A). Finally, length of linked region at greater than 20-fold reductions under the NPL model increased notably and became more sporadic (Figure 5B). A similar pattern was observed under the recessive model (Figure 5C). As SNP number reduction increased and cut off below maximum LOD decreased, it became increasingly probable that the critical region containing *FBXO7*

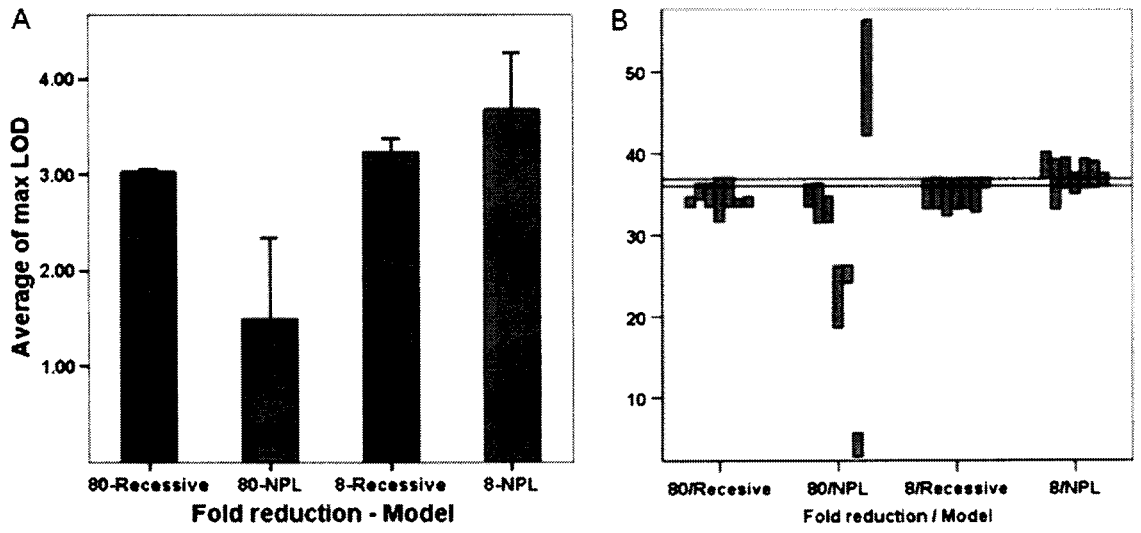

Figure 6. Effects of Change In-Frame of SNP Reductions
(A) Effect on maximum LOD score. Bars indicate ± 1 standard deviation.
(B) Effect on length of linked region. The linked region is defined by cut off of 0.1 below maximum LOD score. The y axis shows cM along chromosome 22. The horizontal grid shows the 36.00–36.88 cM region.

would not be included in selected region under the NPL model (Figure 5B). In addition to these effects, at reductions greater than 20-fold, spurious peaks in other regions of chromosome 22 were observed (not shown).

The 80-fold and 8-fold reduction of SNPs produce, respectively, platforms comparable to 10 K and 100 K chips. In order to consider possible consequence of using different combination of SNPs, these two levels of reductions were each performed in several frames (Figure 6). All seven possible frames for the 8-fold reduction and the first seven frames for the 80-fold reduction were tested. The complement of SNPs included had minimal effects on information content (not shown). The average maximum LOD score for the 8-fold reductions under the NPL and recessive models were 3.68 ± 0.59 and 3.2 ± 0.14, respectively (Figure 6A). The trend of less variation in maximum LOD scores under the recessive model was more notable at 80-fold reductions of SNP numbers. The average maximum LOD scores under NPL and recessive models were, respectively, 1.5 ± 0.84 and 3.0 ± 0.02. Interestingly, the selected 36.00 cM to 36.88 cM region lies within the linked region of all 8-fold reduction frames under the recessive model and within seven of the 8-fold reductions under the NPL model. Among the ten 80-fold reductions tested, the gene lies within the linked area in only two frames under the recessive model and in none under the NPL model. Linked regions were notably sporadic with 80-fold reductions under the NPL model (Figure 6B).

Based on these observations, we conclude that for our pedigree, it may have proved unproductive to use chips containing less than 100,000 SNPs spread across the genome. The conclusion may not be valid for all linkage analysis with single pedigrees, but should be taken into consideration because the costs associated with the use of dense chips has decreased. In linkage analysis with a larger number of pedigrees, the fraction of SNPs that are uninformative because of only one allele being observed throughout the pedigrees is expected to decrease, and chips of less density may perform adequately in such studies.

Supplemental Data

Six figures, three tables, and four movies are available at http://www.ajhg.org/.

Acknowledgments

We thank the patients and their family members for consenting to participate in this study, Kaveh Moini for writing the SNP filtering program, and Ali Katanforoush and Alireza Saleh for computer access. We acknowledge the Iran National Science Foundation; the Center of Excellence in Biomathematics, School of Mathematics, University of Tehran; and Iranian Studies for Parkinson's Disease Grant (5187 Iran PD genetics) for funding this research. All authors declare absence of conflict of interests.

Received: March 27, 2008
Revised: April 27, 2008
Accepted: May 9, 2008
Published online: May 29, 2008

Web Resources

The URLs for data presented herein are as follows:

Berkeley Drosophila Genome Project, http://www.fruitfly.org/seq_tools/splice.html
ClustalW2, http://www.ebi.ac.uk/clustalw

GENSCAN, http://genes.mit.edu/GENSCAN.html
International HapMap Project, http://www.hapmap.org/
Merlin, http://www.sph.umich.edu/csg/abecasis/Merlin/tour/
NCBI, http://www.ncbi.nlm.nih.gov/
Online Mendelian Inheritance in Man (OMIM), http://www.ncbi.nlm.nih.gov/Omim/
SNP filter program, http://www.fos.ut.ac.ir/elahehelahi/Programs/tabid/2964/Default.aspx

References

1. Sheffield, V.C., Weber, J.L., Buetow, K.H., Murray, J.C., Even, D.A., Wiles, K., Gastier, J.M., Pulido, J.C., Yandava, C., and Sunden, S.L. (1995). A collection of tri-and tetranucleotide repeat markers used to generate high quality, high resolution human genomewide linkage maps. Hum. Mol. Genet. *4*, 1837–1844.
2. Weissenbach, J., Gyapay, G., Dib, C., Vignal, A., Morissette, J., Millasseau, P., Vaysseix, G., and Lathrop, M. (1992). A second-generation linkage map of the human genome. Nature *359*, 794–801.
3. Goddard, K.A., and Wijsman, E.M. (2002). Characteristics of genetic markers and maps for cost-effective genome screens using diallelic markers. Genet. Epidemiol. *22*, 205–220.
4. Kruglyak, L. (1997). The use of a genetic map of biallelic markers in linkage studies. Nat. Genet. *17*, 21–24.
5. Matise, T.C., Sachidanandam, R., Clark, A.G., Kruglyak, L., Wijsman, E., Kakol, J., Buyske, S., Chui, B., Cohen, P., and de Toma, C. (2003). A 3.9-centimorgan-resolution human single-nucleotide polymorphism linkage map and screening set. Am. J. Hum. Genet. *73*, 271–284.
6. Wilson, A.F., and Sorant, A.J. (2000). Equivalence of single-and multilocus markers: power to detect linkage with composite markers derived from biallelic loci. Am. J. Hum. Genet. *66*, 1610–1615.
7. Woods, C.G.V.E.M., Bond, J., and Roberts, E. (2004). A new method for autozygosity mapping using single nucleotide polymorphisms (SNPs) and excludeAR. J. Med. Genet. *41*, e101.
8. Abd El-Aziz, M.M., El-Ashry, M.F., Chan, W.M., Chong, K.L., Barragan, I., Antiñolo, G.A., Pang, C.P., and Bhattacharya, S.S. (2006). A novel genetic study of Chinese families with autosomal recessive retinitis pigmentosa. Ann. Hum. Genet. *71*, 281–294.
9. Middleton, F.A., Pato, M.T., Gentile, K.L., Morley, C.P., Zhao, X., Eisener, A.F., Brown, A., Petryshen, T.L., Kirby, A.N., Medeiros, H., et al. (2004). Genomewide linkage analysis of bipolar disorder by use of a high-density single-nucleotide–polymrphism (SNP) genotyping assay: a comparison with microsatellite marker assays and finding of significant linkage to chromosome 6q22. Am. J. Hum. Genet. *74*, 886–897.
10. Paterson, A.D., Wang, X.-Q.L.K., Magistroni, R., Song, X., Kappel, J., Klassen, J., Cattran, D., George-Hyslop, P.S., and Pei, Y. (2007). Genome-wide linkage scan of a large family with IgA nephropathy localizes a novel susceptibility locus to chromosome 2q36. J. Am. Soc. Nephrol. *18*, 2408–2415.
11. Sellick, G.S., Longman, C., Tolmie, J., Newbury-Ecob, R., Geenhalgh, L., Hughes, S., Whiteford, M., Garrett, C., and Houlston, R.S. (2004). Genomewide linkage searches for Mendelian disease loci can be efficiently conducted using high-density SNP genotyping arrays. Nucleic Acids Res. *32*, e164.
12. Vance, C., Al-Chalabi, A., Ruddy, D., Smith, B.N., Hu, X., Sreedharan, J., Siddique, T., Schelhaas, H.J., Kusters, B., Troost, D., et al. (2006). Familial amyotrophic lateral sclerosis with frontotemporal dementia is linked to a locus on chromosome 9p13.2–21.3. Brain *129*, 868–876.
13. Evans, D.M., and Cardon, L.R. (2004). Guidelines for genotyping in genomewide linkage studies: single-nucleotide–polymorphism maps versus microsatellite maps. Am. J. Hum. Genet. *75*, 687–692.
14. Nisipeanu, P.D., and Korczyn, A. (1999). The Parkinsonian-Pyramidal Syndrome. In Movement Disorders in Neurology and Neuropsychiatry, A.B. Joseph and R.R. Young, eds. (Malden, MA: Blackwell Science), pp. 247–250.
15. Kalita, J., Misra, U., and Das, B. (2003). Sporadic variety of pallido-pyramidal syndrom. Neurol. India *51*, 383–384.
16. Panagariya, A., Sharma, B., and Dev, A. (2007). Pallido-Pyramidal syndrome: a rare entity. Indian J. Med. Sci. *61*, 156–157.
17. Sirvastava, T., Goyal, V., Singh, S., Shukla, G., and Behari, M. (2005). Pallido-pyramidal syndrome with blepharospasm and good response to levadopa. J. Neurol. *252*, 1537–1538.
18. Tranchant, C., Boulay, C., and Warter, J. (1991). Le syndrome pallido-pyrimidal: une entité méconnue. Rev. Neurol. *147*, 308–310.
19. Jankovic, J., and Tolosa, E. (2007). Parkinson's Disease & Movement Disorders (Philadelphia: Lippincott Williams & Wilkins).
20. Abecasis, G.R., Cherny, S.S., Cookson, W.O., and Cardon, L.R. (2002). Merlin—rapid analysis of dense genetic maps using sparse gene flow trees. Nat. Genet. *30*, 97–101.
21. Kong, A., and Cox, N. (1997). Allele-sharing models: LOD scores and accurate linkage tests. Am. J. Hum. Genet. *61*, 1179–1188.
22. Lander, E., and Kruglyak, L. (1995). Genetic dissection of complex traits: guidlines for interpreting and reporting linkage results. Nature *11*, 241–247.
23. Apte, S., Olsen, B., and Murphy, G. (1995). The gene structure of tissue inhibitor of metalloproteinases (TIMP)-3 and its inhibitory activities define the distinct TIMP gene family. J. Biol. Chem. *270*, 14313–14318.
24. Ciechanover, A., and Brundin, P. (2003). The ubiquitin proteasome system in neurodegenerative diseases: sometimes the chicken, sometimes the egg. Neuron *40*, 427–446.
25. Hosaka, M., and Südhof, T. (1998). Synapsin III, a novel synapsin with an unusual regulation by Ca^{2+}. J. Biol. Chem. *273*, 13371–13374.
26. Jin, J., Cardozo, T., Lovering, R.C., Elledge, S.J., Pagano, M., and Harper, J.W. (2004). Systematic analysis and nomenclature of mammalian F-box proteins. Genes Dev. *18*, 2573–2580.
27. Kanai, Y., Dohmae, N., and Hirokawa, N. (2004). Kinesin transports RNA: isolation and characterization of an RNA-transporting granule. Neuron *43*, 513–525.
28. Kao, H., Porton, B., Czernik, A., Feng, J., Yiu, G., Häring, M., Benfenati, F., and Greengard, P. (1998). A third member of the synapsin gene family. Proc. Natl. Acad. Sci. USA *95*, 4667–4672.
29. Chang, Y.-F., Cheng, C.-M., Chang, L.-K., Jong, Y.-J., and Yuo, C.-Y. (2006). The F-box protein Fbxo7 interacts with human inhibitor of apoptosis protein cIAP1 and promotes cIAP1 ubiquitination. Biochem. Biophys. Res. Commun. *342*, 1022–1026.

30. Hsu, J.-M., Lee, Y.-C.G., Yu, C.-T.R., and Huang, C.-Y.F. (2004). Fbx7 functions in the SCF complex regulating Cdk1-Cyclin B-phosphorylated hepatoma up-regulated protein (HURP) proteolysis by a proline-rich region. J. Biol. Chem. *279*, 32592–32602.
31. Laman, H. (2006). Fbxo7 gets proactive with cyclin D/cdk6. Cell Cycle *5*, 279–282.
32. Bai, C., Sen, P., Mathias, N., Hofmann, K., Ma, L., Goebl, M., Harper, J., and Elledge, S. (1996). SKP1 connects cell cycle regulators to the ubiquitin proteolysis machinery through a novel motif, the F-box. Cell *86*, 263–274.
33. Cenciarelli, C., Chiaur, D.S., Guardavaccaro, D., Parks, W., Vidal, M., and Pagano, M. (1999). Identification of a family of human F-box proteins. Curr. Biol. *9*, 1177–1179.
34. Winston, J.T., Koepp, D.M., Zhu, C., Elledge, S.J., and Harper, J.W. (1999). A family of mammalian F-box proteins. Curr. Biol. *9*, 1180–1182.
35. Laman, H., Funes, J.M., Ye, H., Henderson, S., Galinanes-Garcia, L., Hara, E., Knowles, P., McDonald, N., and Boshoff, C. (2005). Transforming activity of Fbxo7 is mediated specifically through regulation of cyclin D/cdk6. EMBO J. *24*, 3104–3116.
36. Haglund, K., and Dikic, I. (2005). Ubiquitylation and cell signaling. EMBO J. *24*, 3353–3359.
37. Shcherbik, N., and Haines, D. (2004). Ub on the move. J. Cell. Biochem. *93*, 11–19.
38. Huang, Q., Shete, S., and Amos, C.I. (2004). Ignoring linkage disequilibrium among tightly linked markers induces false-positive evidence of linkage for affected sib pair analysis. Am. J. Hum. Genet. *75*, 1106–1112.
39. Schaid, D.J., McDonnell, S.K., Wang, L., Cunningham, J.M., and Thibodeau, S.N. (2002). Caution on pedigree haplotype inference with software that assumes linkage equilibrium. Am. J. Hum. Genet. *71*, 992–995.
40. Consortium, T.A.G.P. (2007). Mapping autism risk loci using genetic linkage and chromosomal rearrangements. Nat. Genet. *39*, 319–328.
41. Levinson, D.F., and Holmans, P. (2005). The effect of linkage disequilibrium on linkage analysis of incomplete pedigrees. BMC Genet. *6*, S6.

OPEN ACCESS Freely available online

PLoS one

Loss of Nuclear Activity of the FBXO7 Protein in Patients with Parkinsonian-Pyramidal Syndrome (PARK15)

Tianna Zhao[1], Esther De Graaff[1¤], Guido J. Breedveld[1], Agnese Loda[1], Lies-Anne Severijnen[1], Cokkie H. Wouters[1], Frans W. Verheijen[1], Marieke C. J. Dekker[2], Pasquale Montagna[3], Rob Willemsen[1], Ben A. Oostra[1], Vincenzo Bonifati[1]*

1 Department of Clinical Genetics, Erasmus MC, Rotterdam, The Netherlands, **2** Department of Neurology, Radboud University Medical Center, Nijmegen, The Netherlands, **3** Department of Neurology, University of Bologna, Bologna, Italy

Abstract

Mutations in the *F-box only protein 7* gene (*FBXO7*) cause PARK15, an autosomal recessive neurodegenerative disease presenting with severe levodopa-responsive parkinsonism and pyramidal disturbances. Understanding the PARK15 pathogenesis might thus provide clues on the mechanisms of maintenance of brain dopaminergic neurons, the same which are lost in Parkinson's disease. The protein(s) encoded by *FBXO7* remain very poorly characterized. Here, we show that two protein isoforms are expressed from the *FBXO7* gene in normal human cells. The isoform 1 is more abundant, particularly in primary skin fibroblasts. Both isoforms are undetectable in cell lines from the PARK15 patient of an Italian family; the isoform 1 is undetectable and the isoform 2 is severely decreased in the patients from a Dutch PARK15 family. In human cell lines and mouse primary neurons, the endogenous or over-expressed, wild type FBXO7 isoform 1 displays mostly a diffuse nuclear localization. An intact N-terminus is needed for the nuclear FBXO7 localization, as N-terminal modification by PARK15-linked missense mutation, or N-terminus tag leads to cytoplasmic mislocalization. Furthermore, the N-terminus of wild type FBXO7 (but not of mutant FBXO7) is able to confer nuclear localization to profilin (a cytoplasmic protein). Our data also suggest that overexpressed mutant FBXO7 proteins (T22M, R378G and R498X) have decreased stability compared to their wild type counterpart. In human brain, FBXO7 immunoreactivity was highest in the nuclei of neurons throughout the cerebral cortex, intermediate in the globus pallidum and the substantia nigra, and lowest in the hippocampus and cerebellum. In conclusion, the common cellular abnormality found in the PARK15 patients from the Dutch and Italian families is the depletion of the FBXO7 isoform 1, which normally localizes in the cell nucleus. The activity of FBXO7 in the nucleus appears therefore crucial for the maintenance of brain neurons and the pathogenesis of PARK15.

Citation: Zhao T, De Graaff E, Breedveld GJ, Loda A, Severijnen L-A, et al. (2011) Loss of Nuclear Activity of the FBXO7 Protein in Patients with Parkinsonian-Pyramidal Syndrome (PARK15). PLoS ONE 6(2): e16983. doi:10.1371/journal.pone.0016983

Editor: Eric Kremer, French National Centre for Scientific Research, France

Received September 7, 2010; **Accepted** January 19, 2011; **Published** February 11, 2011

Funding: This work was supported by the Erasmus MC Rotterdam (Erasmus Fellowship), and the Netherlands Organization for Scientific Research (NWO, VIDI grant) to VB. The funders had no role in study design, data collection and analysis, decision to publish, or preparation of the manuscript.

Competing Interests: The authors have declared that no competing interests exist.

* E-mail: v.bonifati@erasmusmc.nl

¤ Current address: Department of Neurosciences, Erasmus MC, Rotterdam, The Netherlands

Introduction

Parkinson's disease (PD), the second most common neurodegenerative disorder after Alzheimer's disease, is pathologically characterized by the progressive loss of dopaminergic neurons in the substantia nigra of the midbrain, and the formation of alpha-synuclein-containing protein aggregates, termed Lewy bodies, in surviving neurons [1]. In recent years, defective ubiquitin-proteasome system, mitochondrial dysfunction, oxidative stress, and autophagy impairment have all been suggested to play some roles in the PD pathogenesis, but the primary molecular mechanisms of this disease remain mostly unknown [2,3]. PD is a sporadic, idiopathic disorder in most patients, but the identification of genetic mutations causing rare Mendelian forms of parkinsonism has provided novel clues for understanding of the disease pathogenesis [3,4]. Some of these Mendelian parkinsonism, such as those caused by dominant mutations in the *alpha-synuclein* (PARK1) or *leucine-rich repeat kinase 2* (PARK8) gene, are more similar to the common, idiopathic PD form [5]. In other forms, such as those caused by recessive mutations in the *parkin* (PARK2), *PINK1* (PARK6), *DJ-1* (PARK7), and *ATP13A2* (PARK9), the phenotype is more often atypical due to younger-onset, presence of additional clinical signs (dementia, pyramidal signs), or absence of Lewy body-pathology [6,7,8]. However, despite these atypical phenotypes, understanding the mechanisms of the Mendelian parkinsonisms might provide important clues into the pathways leading to the degeneration of the dopaminergic neurons, which might also be involved in the common forms of PD. For example, the ATP13A2 protein has been recently identified as a potent modifier of the toxicity induced by alpha-synuclein in animal models of PD [9].

Recently, we characterized mutations in the *F-box only protein 7* (*FBXO7*) gene, encoding the F-box protein 7 (FBXO7), as the cause of PARK15, an autosomal recessive neurodegenerative disease presenting with juvenile, severe levodopa-responsive parkinsonism and additional pyramidal signs [10]. A homozygous

FBXO7 nonsense mutation (R498X) is present in an Italian family, while compound heterozygous mutations (IVS7+1G/T and a T22M mutation) are found in a Dutch family. Another homozygous mutation (R378G) was previously identified by others in an Iranian family [11].

FBXO7 is a member of the F-box-containing protein (FBP) family, characterized by a ~40-amino acids domain (the F-box) [12,13,14]. FBPs serve as molecular scaffolds in the formation of protein complexes, and have been implicated in a range of processes, such as cell cycle, genome stability, development, synapse formation, and circadian rhythms (reviewed in [15]). Through the interaction between the F-box and the Skp1 protein, FBPs might become part of SCF (Skp1, Cullin1, F-box protein) ubiquitin ligase complexes, and play roles in ubiquitin-mediated proteasomal degradation [15]. However, FBPs might also be involved in ubiquitin-mediated, non-proteasomal pathways, and SCF-independent non-proteolytic functions [15].

Two *FBXO7* transcript variants are annotated in Genbank (accession number NM_012179.3 and NM_001033024.1), resulting from the usage of different open reading frame (ORF) start codons on alternatively spliced 5'-exons, and predicted to encode two FBXO7 protein isoforms of 522 and 443 amino acids (also referred to as isoform 1 and isoform 2). However, the experimental confirmation of the existence of these two protein isoforms has remained elusive. Nothing is known about the expression of the FBXO7 protein(s) in the human brain.

The FBXO7 isoform 1 is longer than isoform 2 because of the presence of an N-terminal ubiquitin-like (Ubl) domain (absent in the isoform 2), which is thought to interact with ubiquitin receptor proteins (Figure 1). The remaining domains are present in both isoforms, including an FP (FBXO7/PI31) domain, the F-box motif, and a C-terminal proline-rich region (PRR). The FP domain mediates the interaction of FBXO7 with the proteasome inhibitor protein PI31 [16]. The PRR appears crucial for the binding of FBXO7 to its reported substrates.

Very little is known about the function and the sub-cellular localization of these two FBXO7 proteins. FBXO7 has been reported to interact with the hepatoma up-regulated protein (HURP, a mitotic protein) [17], the inhibitor of apoptosis protein 1 (cIAP1) [18], and the proteasome inhibitor protein PI31 [16]. Last, FBXO7 was shown to possess SCF-independent transforming activity by enhancing the interaction of cyclin-dependent-kinase CDK6 with its targets [19]. Whether these or other still unknown FBXO7 interacting-proteins are important for the

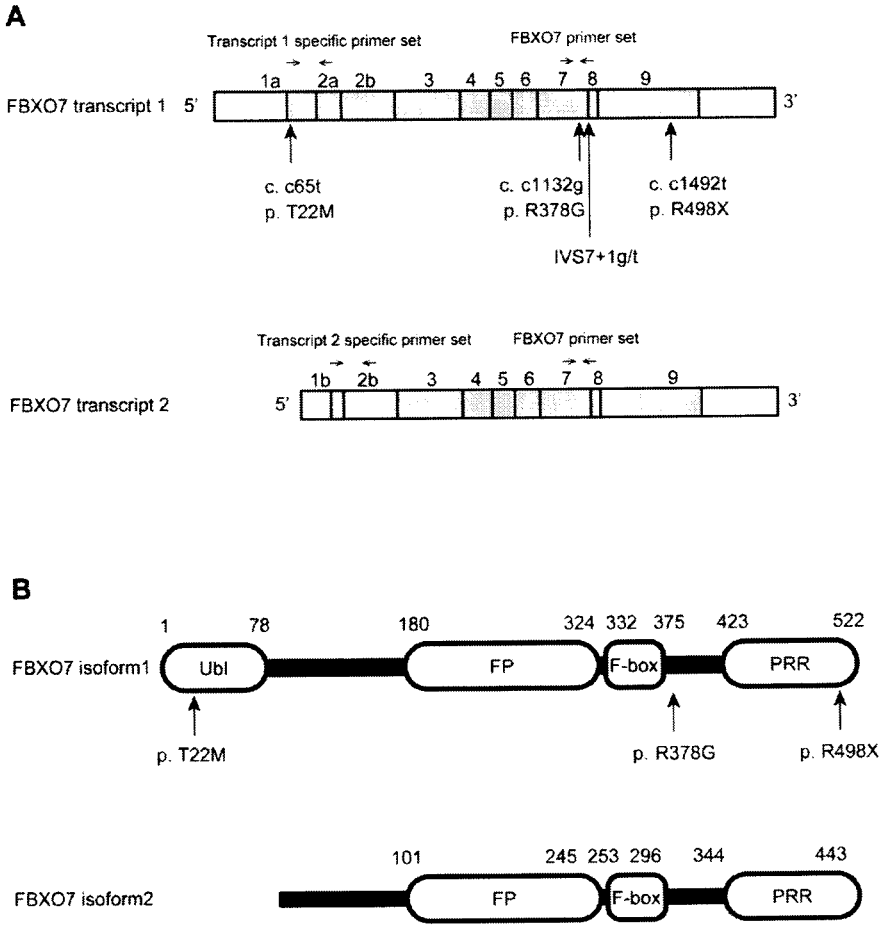

Figure 1. Schematic representation of the *FBXO7* transcripts and protein isoforms. (A) The *FBXO7* transcripts with location of the mutations found in patients with PARK15. The location of the primers used in qPCR is indicated by arrows. (B) Domain organization of the two FBXO7 protein isoforms. Ubl: ubiquitin-like domain; FP: FBXO7/ PI31 domain; F-box: F-box motif; PRR: proline rich domain.
doi:10.1371/journal.pone.0016983.g001

neuronal function of FBXO7 and for the mechanisms of neurodegeneration remains unknown. Here, we show the existence of two FBXO7 protein isoforms in normal human cells; we characterize their subcellular localization and their differential depletion in cell lines from the patients with PARK15; last, we characterize the expression of the FBXO7 proteins in the normal human brain.

Results

Expression of the FBXO7 proteins in families with PARK15

To study the expression of the endogenous FBXO7 proteins, we obtained Epstein-Barr virus (EBV)-transformed lymphoblastoid cell lines from members of the Italian and Dutch PARK15 families, and from unrelated normal controls. Fibroblast lines were also established from skin biopsies in one Dutch PARK15 patient and one unrelated control. Unfortunately, fibroblasts from the second Dutch PARK15 patient and from patients of the Italian PARK15 family were not available.

In lymphoblastoid cells from normal controls (Figures 2 and 3), and HEK 293T cells (Figure S1), our Western blot (WB) analysis using an antibody against FBXO7 revealed two bands of the expected molecular weight of the FBXO7 isoform 1 and isoform 2. The knock down (KD) of *FBXO7* gene in HEK 293T cells confirmed the specificity of the antibody for the FBXO7 proteins (Figure S1).

In the Dutch family, two siblings were affected by PARK15 and they carried compound heterozygous *FBXO7* mutations: the splice-site mutation IVS7+1G/T, which removes the invariable splice donor of intron 7 and is expected to disrupt the splicing of both the *FBXO7* transcript isoforms; and a substitution in exon 1A, c.C65T, predicted to lead to the missense change p.T22M, but only in the longer FBXO7 protein isoform 1 (Figure 2A). We previously documented the expression of both *FBXO7* alleles in these patients, by verifying the presence of the heterozygous c.C65T mutation in cDNA from blood cells [10]. We also showed multiple aberrantly spliced transcripts resulting from the activation of cryptic splice sites in exon 7, and encoding frame-shift proteins followed by premature truncation [10]. These are usually unstable and rapidly degraded by the cell.

In the Dutch PARK15 patients, the FBXO7 isoform 1 was undetectable in WB, while the isoform 2 was detected in lower amounts (Figure 2C). The unaffected mother (NIJ-001) who only carried the T22M mutation, showed lower amount of the isoform

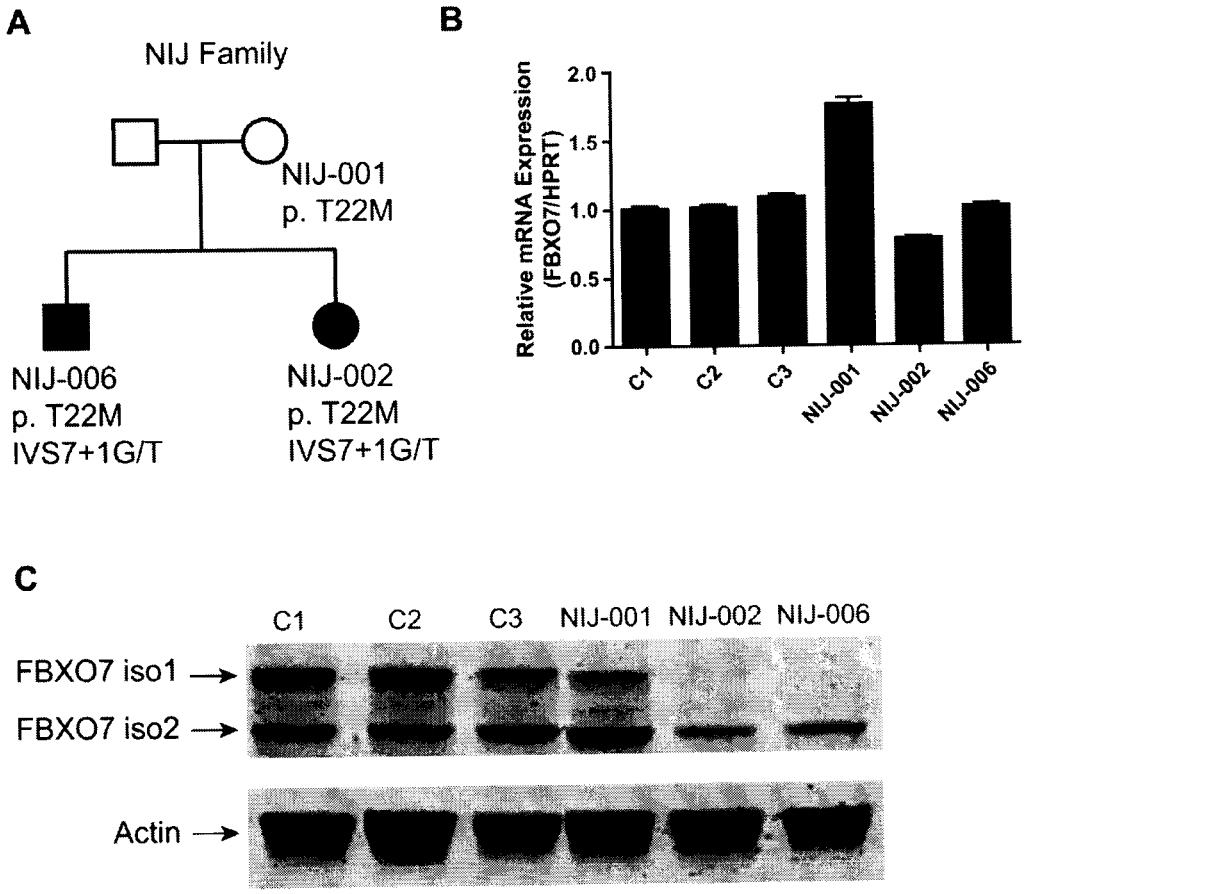

Figure 2. Expression of FBXO7 in the Dutch PARK15 family. (A) Family pedigree and *FBXO7* genotypes. (B) qPCR analysis of *FBXO7* mRNA (both transcript isoforms) in members of the PARK15 family and unrelated, healthy controls (C1–C3). (C) Western blotting analysis. The two FBXO7 isoforms present in controls are altered in the mutation carriers. The isoform 1 is undetectable in the patients (NIJ-002 and NIJ-006) and decreased in the mother (NIJ-001), who also carries the mutation affecting this isoform (T22M). The isoform 2 is decreased in the patients and normal in the mother (see text for further details).
doi:10.1371/journal.pone.0016983.g002

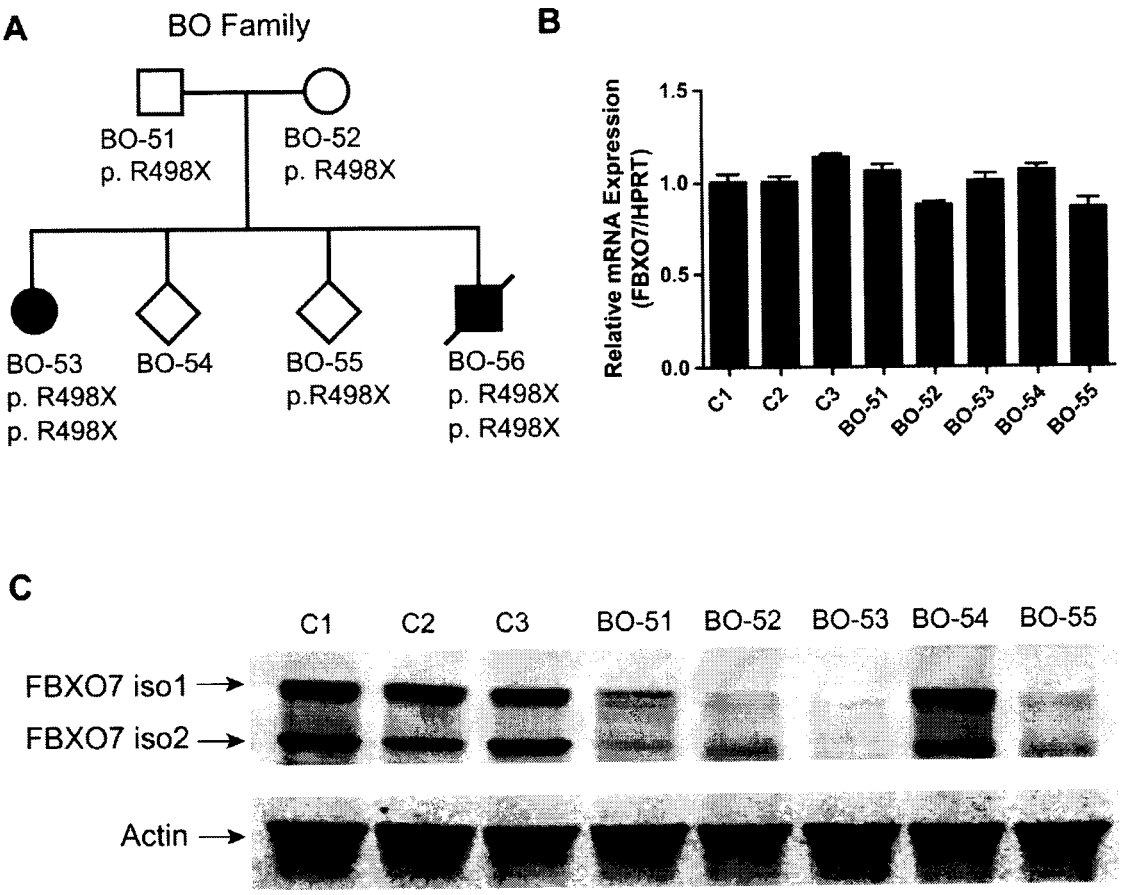

Figure 3. Expression of FBXO7 in the Italian PARK15 family. (A) Family pedigree and *FBXO7* genotypes. (B) qPCR analysis of *FBXO7* mRNA (both transcript isoforms) in members of the PARK15 family and unrelated, healthy controls (C1–C3). (C) Western blotting analysis. The two FBXO7 isoforms present in controls are both undetectable in the PARK15 patient (BO-53), and markedly decreased in the heterozygous mutation carriers (BO-51, BO-52, BO-55). The BO-54 subject is not a carrier of the mutation and shows normal FBXO7 expression.
doi:10.1371/journal.pone.0016983.g003

1, and normal amount of isoform 2. These results are compatible with lack of FBXO7 protein expression from the allele containing the IVS7+1G/T mutation, and with only isoform 2 being expressed from the allele containing the T22M mutation. In other words, the T22M mutation leads to selective depletion of the isoform 1, the only isoform in which this mutation is incorporated.

To exclude effects of these mutations at mRNA level, or presence of other, unknown mutations in linkage disequilibrium, we performed quantitative PCR (qPCR) analysis of the total FBXO7 transcripts, as well as the isoform 1-specific and the isoform 2-specific transcripts separately. These experiments showed that the *FBXO7* mRNA levels in the Dutch patients were similar to those in unrelated controls (Figure 2B and Figure S3), suggesting that the main effect of these mutations is at the level of protein stability.

The two affected siblings in the Italian PARK15 family carry an *FBXO7* homozygous nonsense mutation in exon 9, predicted to affect both transcripts (c.C1492T, according to the longer *FBXO7* transcript, protein effect p.R498X) (Figure 3A). qPCR analysis showed similar *FBXO7* mRNA levels among unrelated healthy controls, R498X heterozygous and homozygous mutation carriers (Figure 3B and Figure S3), indicating that this truncating mutation escapes nonsense-mediated mRNA decay [20]. However, in WB analysis, the R498X heterozygous carriers displayed reduced levels of both the FBXO7 protein isoforms, while the FBXO7 proteins were both undetectable in the homozygous PARK15 patient (Figure 3C). Unfortunately, the second patient in this family died before cell lines could be obtained. Thus, in the case of this nonsense mutation, the main final effect is the depletion of both FBXO7 protein isoforms, likely due to protein instability. Since this mutation only removes the last 24 residues of FBXO7, the C-terminus appears therefore very important for the stability of this protein.

Subcellular localization of wild type and mutant FBXO7

To investigate the subcellular localization of FBXO7, we transiently transfected HEK 293T cells with plasmids overexpressing the wild type (WT) or mutant FBXO7 isoform 1. Forty-eight hours after transfection we analyzed the cells by immunofluorescence and confocal microscopy. In mock transfected HEK 293T cells, a main nuclear and much weaker cytosolic staining was observed (Figure 4A). *FBXO7* stable knock-down in these cells confirmed the specificity of the staining, which represents therefore the endogenous FBXO7 protein (Figure S2). The overexpression of the WT FBXO7 isoform 1 in HEK 293T cells resulted in a mostly nuclear staining, a pattern shared by the R378G mutant

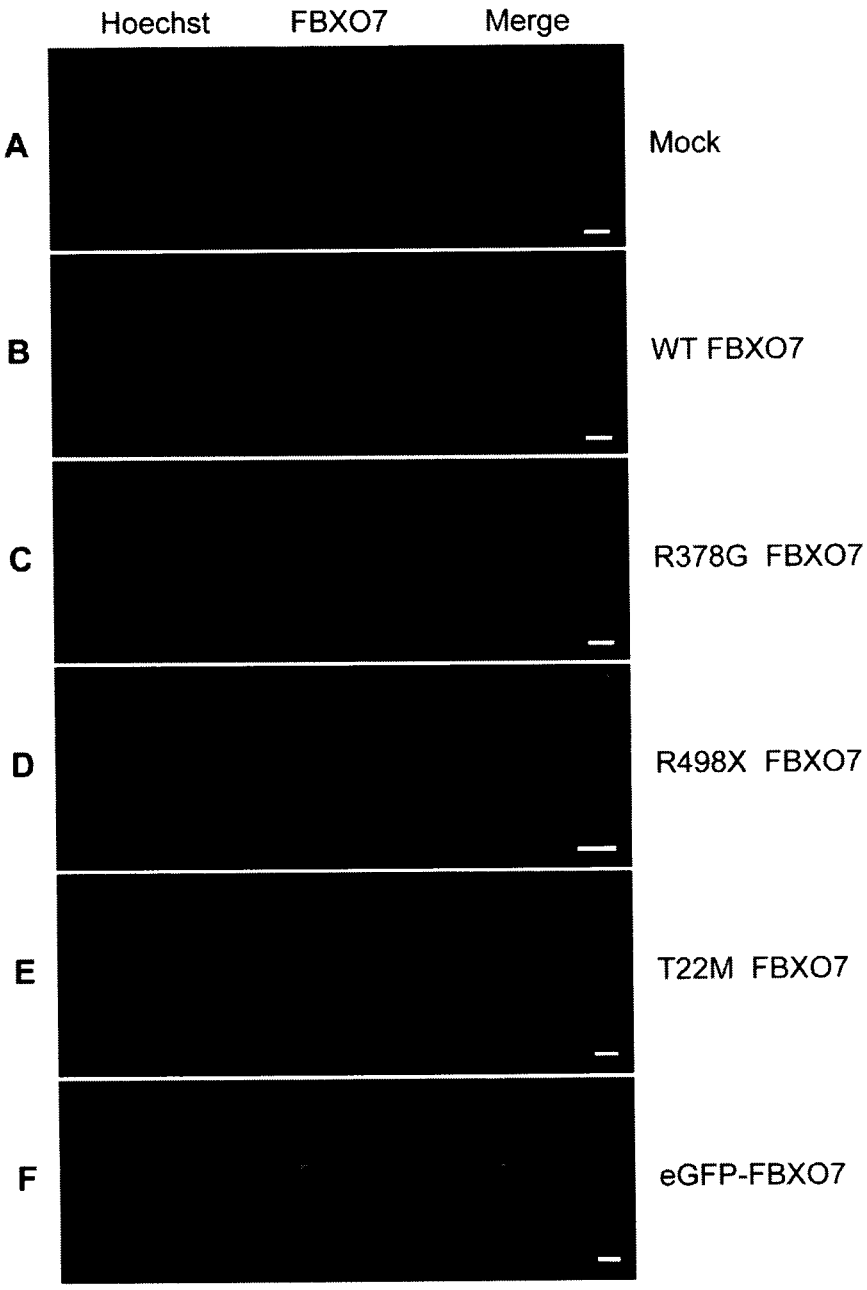
Hoechst
FBXO7
Merge
A
Mock
B
WT FBXO7
C
R378G FBXO7
D
R498X FBXO7
E
T22M FBXO7
F
eGFP-FBXO7

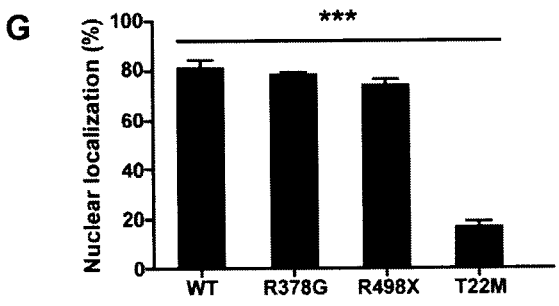
G
***
Nuclear localization (%)
100
80
60
40
20
0
WT
R378G
R498X
T22M

Figure 4. Localization of FBXO7 in HEK 293T cells. Cells were transfected with empty vector (mock, A), wild type *FBXO7* (B), R378G mutant (C), R498X mutant (D), T22M mutant (E) and N-terminus-tagged *eGFP-FBXO7* (F). In panels A–E, the FBXO7 protein is visualized in red by using a mouse primary anti-FBXO7 antibody and a Cy3-coupled secondary anti-mouse antibody. In panel F, the FBXO7 protein is directly visualized by the green eGFP signal. The nucleus (Hoechst staining) is depicted in green, with the exception of panel F, where it is stained in blue (scale bars, 10 μm). (G) Quantification of the nuclear localization of FBXO7. At least 200 HEK 293T cells expressing FBXO7 were counted. *** $p<0.01$ (chi-square test - T22M versus wild type and other FBXO7 variants).
doi:10.1371/journal.pone.0016983.g004

(Figure 4B and Figure 4C). A much weaker signal was still diffusely detected in the cytoplasm.

To confirm the localization of endogenous wild type and mutant FBXO7, we performed immunofluorescence in fibroblasts from one Dutch PARK15 patient, and one unrelated normal control (Figure 5). A pattern of mainly nuclear fluorescence (similar to that seen in HEK 293T cells in Figure 4A) was often observed in the control fibroblasts, but never in the patient fibroblasts (Figure 5). WB analysis confirmed the expression of two FBXO7 isoforms in normal fibroblasts (Figure 5D); compared with

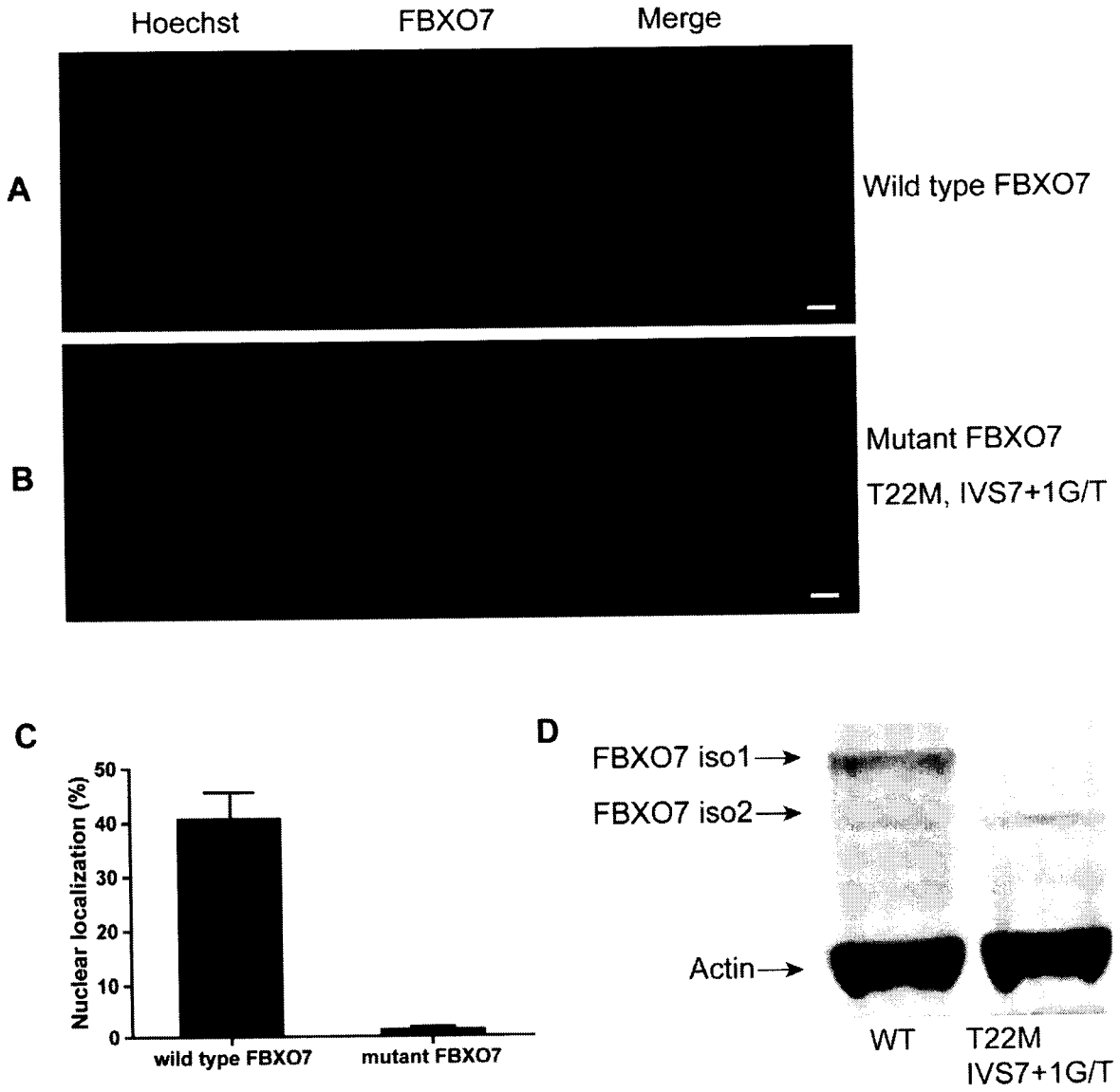

Figure 5. Expression of endogenous FBXO7 in human fibroblasts. (A, B) For immunofluorescence, the FBXO7 protein is visualized in red by using a mouse primary anti-FBXO7 antibody and a Cy3-coupled secondary anti-mouse antibody. The nucleus (Hoechst staining) is depicted in green. (scale bars, 10 μm). (A) normal control; (B) Dutch PARK15 patient with T22M and IVS7+1G/T mutations. (C) quantification of percentages of cells showing mainly nuclear localization of FBXO7. (D) Western blotting analysis of fibroblasts from a normal control and the Dutch PARK15 patient.
doi:10.1371/journal.pone.0016983.g005

lymphoblasts, here the isoform 1 was much more abundant than isoform 2. In the fibroblasts from the Dutch PARK15 patient, the isoform 1 was undetectable by WB, while isoform 2 was detected, in agreement with the results of WB in lymphoblastoid cells from the same patient (Figure 2C). Taken together, the experiments in the patients fibroblasts show that the loss of isoform 1 (WB) is associated with the loss of immunoreactivity in the nucleus (seen in immunofluorescence). The weak cytosolic immunoreactivity is compatible with the residual expression of isoform 2 seen in this patient in WB.

The FBXO7 R498X mutant displayed an abnormal pattern consisting of diffuse nuclear and cytosolic localization when overexpressed in HEK 293T cells (Figure 4D). Last, the T22M mutant showed the most striking aberrant pattern of mostly cytosolic localization (Figure 4E and Figure 4G). The T22M mutation is close to the N-terminus where it might impair a nuclear localization signal. To test this hypothesis, we overexpressed WT FBXO7 with an N-terminal tag (enhanced green fluorescent protein, eGFP). As expected, the N-terminal tagging totally blocked the nuclear localization of the protein (Figure 4F), mimicking the pattern of the T22M mutant. Furthermore, the first 40 amino acids of WT or T22M-mutant FBXO7 isoform 1 were cloned in front of the mCherry-labeled profilin, a well-known cytosolic protein. As a result, the WT FBXO7 N-terminal 40 amino acid peptide, but not the T22M-mutant, was able to change the localization of profilin from cytoplasm to nucleus (Figure 6).

The localization pattern of WT- and mutant FBXO7 proteins in human neuroblastoma SH-SY5Y cells and mouse primary hippocampal neurons were similar to those described in HEK 293T cells (Figure 7A–I).

Stability of mutant FBXO7 *in vitro*

On the basis of the WB and qPCR observations on the cells from the PARK15 patients, we hypothesized that the missense and nonsense mutants (T22M and R498X) markedly decreased the stability of FBXO7.

To test this hypothesis, the WT and mutant *FBXO7* (T22M and R498X) were transfected in HEK 293T cells. The R378G mutant reported previously in an Iranian PARK15 family [11] was also tested. The overexpression of all these FBXO7 mutants yielded consistently and significantly decreased levels in WB compared with their WT counterpart (Figure 8A–B). This is consistent with our observations in the patients cells and suggest that the FBXO7 mutants are rapidly degraded. To explore the degradation pathways of FBXO7, the lysosomal inhibitor NH_4Cl or the proteasome inhibitor MG-132 were added to the cells overexpressing WT and mutant FBXO7. Treatment with NH_4Cl strongly inhibited the degradation of FBXO7, increasing the steady-state protein expression by three to four fold (Figure 8C–D), which suggests that overexpressed FBXO7 is mainly degraded by the lysosomal pathway. The treatment with MG-132 leads to smaller increases in steady-state FBXO7 expression (Figure 8E–F), indicating a minor role of the proteasome degradation pathway. To control for the transfection efficiency, the WT and mutant *FBXO7* (T22M, R378G, and R498X) were transfected in HEK 293T cells together with the eGFP protein. Similar results were obtained (Figure S4).

FBXO7 proteins expression in the human brain

To characterize the expression of the FBXO7 proteins in the human brain, we studied the following brain regions by immunohistochemistry: frontal, temporal, and occipital cerebral

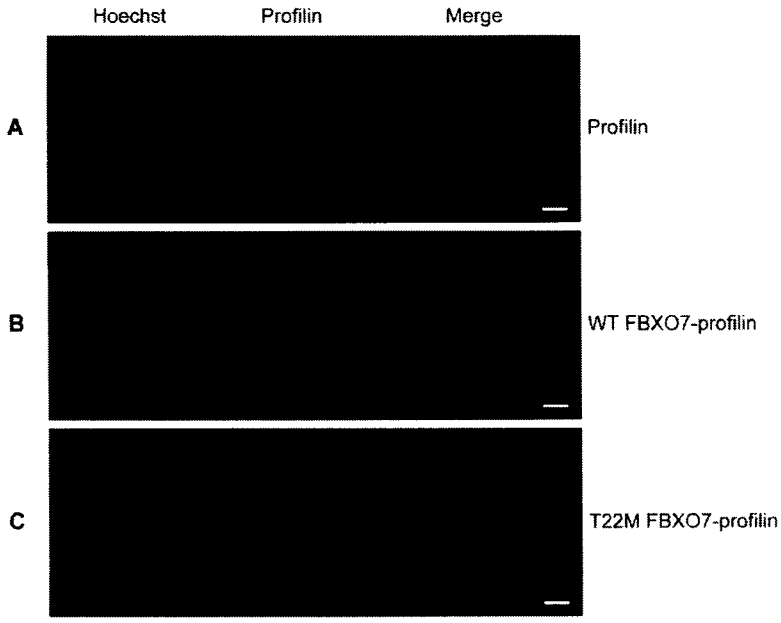

Figure 6. The N-terminus of FBXO7 confers nuclear localization to profilin. In panel (A), Profilin, a well-known cytosolic protein, is visualized by the red mCherry signal; the nucleus is depicted in green (Hoechst staining). Expressing the first 40 amino acids of WT-FBXO7 isoform 1 in front of mCherry-labeled profilin changes the localization of profilin from the cytoplasm to the nucleus (B). The same FBXO7 N-terminal peptide carrying the T22M-mutation found in PARK15 patients is totally devoid of this capacity (C). (scale bars, 10 μm).
doi:10.1371/journal.pone.0016983.g006

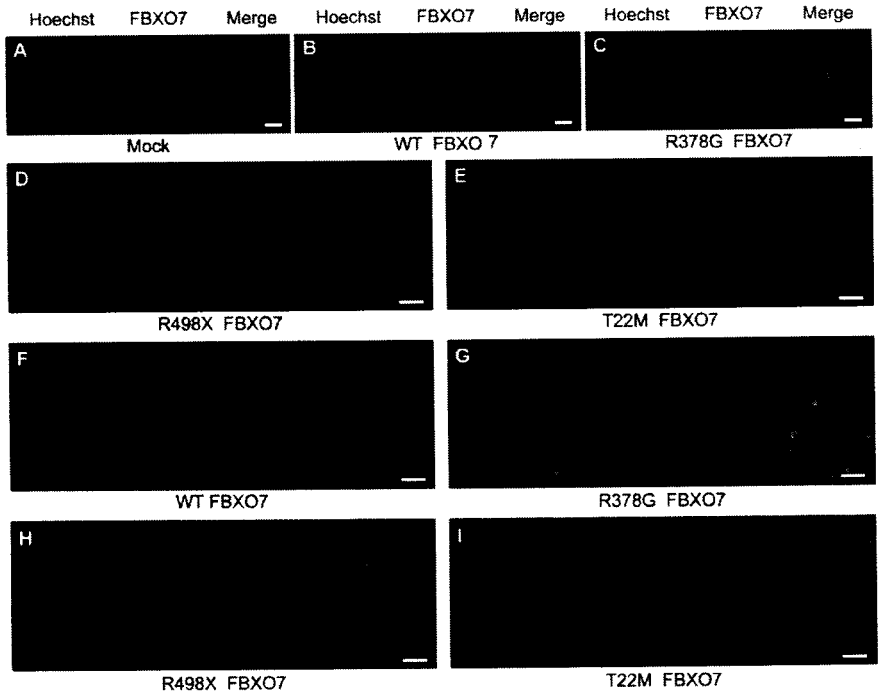

Figure 7. Localization of FBXO7 in SH-SY5Y cells and primary hippocampal neurons. Neuroblastoma SH-SY5Y cells (A–E) and mouse primary hippocampal neurons (F–I) were transfected with empty vector (mock, A), wild type FBXO7 (B, F), R378G mutant (C, G), R498X mutant (D, H), and T22M mutant (E, I) FBXO7. The FBXO7 protein is visualized in red by using a mouse primary anti-FBXO7 antibody and a Cy3-coupled secondary anti-mouse antibody. The nucleus (Hoechst staining) is depicted in green. (scale bars, 20 μm).
doi:10.1371/journal.pone.0016983.g007

cortex, hippocampus, globus pallidum, substantia nigra, and cerebellar cortex. The immunoreactivity was highest in the nuclei of neurons throughout the cerebral cortex, intermediate in neurons in the globus pallidum and the substantia nigra, and lowest in the hippocampus (Figure 9) and cerebellar cortex (not shown).

Discussion

Recessive *FBXO7* mutations are definitely established as the cause of PARK15, a novel form of juvenile neurodegenerative parkinsonism with additional pyramidal signs [10,11]. However, very little is known about the biology of the FBXO7 proteins. Even the existence of the two protein isoforms remained to be confirmed, the subcellular localization was poorly characterized, and the expression in the human brain unexplored. A localization of overexpressed FBXO7 to the cytoplasm and nucleus has been reported in previous studies which all used N-terminal tags to visualize FBXO7 (mostly isoform 1), and did not control for tag-related effects [16,18,19]. The N-terminal tagging was probably responsible for the observed cytosolic localization of FBXO7 in those studies. The localization of the over-expressed untagged FBXO7 or of the endogenous FBXO7 was not previously investigated. This uncertainty in the subcellular localization of the FBXO7 protein also complicates the interpretation of the biological plausibility of the reported interactions with other proteins. On the other hand, it is crucial to assess whether the FBXO7 disease-causing mutations affect protein stability, before these mutants are used in functional studies and conclusions are made about possible pathogenetic mechanisms.

A first important message of this study is that two FBXO7 protein isoforms are expressed in normal human cells. This contention is supported by the fact that the two FBXO7 immunoreactive bands are both undetectable in HEK 293T cells with stable *FBXO7* gene KD, and in the cells from the patients with PARK15 who carry a homozygous truncating mutation predicted to affect both the *FBXO7* transcripts. In keeping with this model, only the FBXO7 isoform 1 is markedly depleted in the Dutch patients, as one of the mutations present in those patients (T22M) is indeed only affecting the isoform 1, leaving the isoform 2 unaffected. Thus, the Dutch patients are still able to express the isoform 2 from this mutant allele, while the other allele (carrying the IVS7+1G/T splice mutation) disrupts the expression of both isoforms. Interestingly, the heterozygous mutation carriers of the Italian family, who display lower levels of both FBXO7 isoforms, remain healthy (Figure 3). On the contrary, the Dutch patients, who still express low levels of only the isoform 2, are affected (Figure 2). This strongly suggests that the depletion of the isoform 1 is the culprit for the pathogenesis of PARK15.

Furthermore, we show that the overexpressed, untagged FBXO7 isoform 1 and also the endogenous FBXO7 protein are mostly localized to the cell nucleus in two human cell models (HEK 293T and SH-SY5Y), as well as in mouse primary hippocampal neurons and human skin fibroblasts. We also show that an intact N-terminus is essential for proper nuclear localization of FBXO7 isoform 1. Modifications in this region of FBXO7, including the missense T22M mutation or N-terminal tagging by eGFP, lead to mislocalization to the cytoplasm. These observations also support the contention that previous reports of cytoplasmic localization of FBXO7 are probably due to N-terminal tagging.

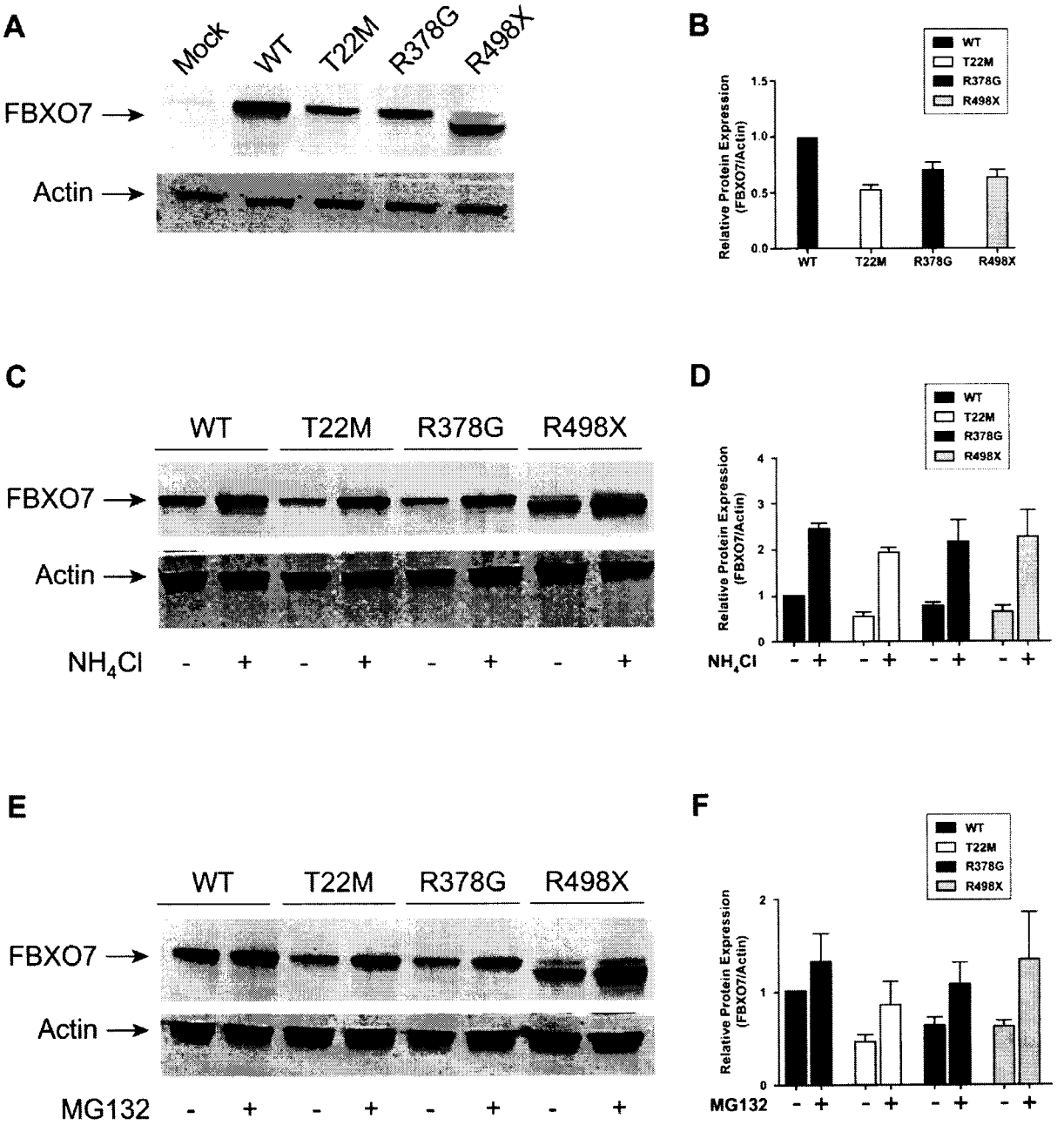

Figure 8. Overexpression of wild type and mutant FBXO7. Overexpression of wild type and mutant FBXO7 proteins in HEK 293T cells (A), and effect of the treatment with the lysosomal inhibitor NH_4Cl (C) and the proteasomal inhibitor MG-132 (E). Actin is used as loading control. The quantification of the protein levels is shown in the right panels (B, D, and F) (Odyssey software).
doi:10.1371/journal.pone.0016983.g008

Canonical nuclear localization signals are not present in the N-terminus of FBXO7. However, nucleus localization signals might also consist of one or more short sequences of positively charged lysine or arginine residues, which are indeed present in the N-terminus of FBXO7 (Figure S5) [21,22]. The effects of N-terminal tagging would therefore be explained by the masking of these signals. How the T22M mutation prevents the nuclear localization of overexpressed FBXO7 is unclear, but the mutation might affect the interaction with other proteins which are crucial for the nuclear import of FBXO7. In support of this contention, we showed that the first 40 amino acids of FBXO7 isoform 1 are crucial for nuclear localization, as they efficiently direct profilin (a cytosolic protein) to the nucleus; however, the T22M mutation suppresses this effect. The C-terminus of the protein might also contain important motifs for nuclear import or export, as the overexpressed R498X mutant also displays an

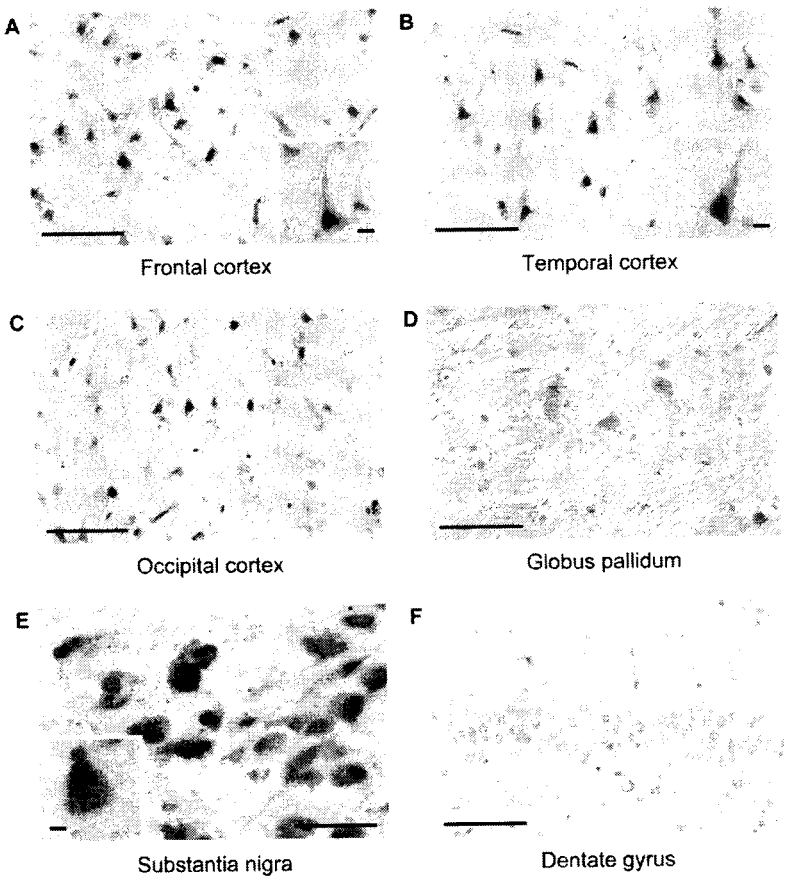

Figure 9. Expression of the FBXO7 protein in the normal human brain. Brain sections are stained using anti-FBXO7 antibody (Abnova): frontal (A), temporal (B), and occipital (C) cortex; globus pallidum (D); substantia nigra (E); dentate gyrus of hippocampus (F). (scale bars, 100 μm).
doi:10.1371/journal.pone.0016983.g009

abnormal pattern of equally diffuse, cytosolic and nuclear localization.

Regarding the stability of the FBXO7 missense and truncated proteins encoded by the mutations causing PARK15, our data collectively suggest that the T22M, R378G and R498X mutants are all significantly unstable compared with the WT protein, at least in our overexpressing systems (Figure 8 and Figure S4). It is possible that the overexpressed FBXO7 mutants were insoluble and therefore not present in the cell lysate fraction. We therefore detected FBXO7 in insoluble fractions, but the amount of FBXO7 mutants was still lower than that of the WT counterpart (data not shown). Furthermore, formation of inclusions or membrane association of overexpressed FBXO7 was not observed. Last, we showed that the overexpressed WT and mutant FBXO7 are mainly degraded via the lysosomal pathway, with also a minor role of the proteasome pathway. Our data also suggest that the overexpressed R378G mutant is less stable than the WT FBXO7. The Iranian PARK15 patients might thus also suffer a severe depletion of the endogenous protein. It will be of interest to test this prediction in patients-derived cells, since we found that R378G does not significantly alter the nuclear localization in transfected cells. If sufficiently stable, this mutant protein could provide important clues about the nuclear function of FBXO7 that is lost in PARK15.

Last, we provide the initial characterization of the expression of the FBXO7 proteins in the normal human brain by immunohistochemistry. The nuclei of neurons throughout the cerebral cortex showed the strongest FBXO7 immunoreactivity, followed by the neurons in the subcortical diencephalic region, and the substantia nigra, while the lowest immunoreactivity was detected in the hippocampus and the cerebellar cortex (Figure 9 and data not shown).

Limited data on the expression of the *FBXO7* gene at mRNA level were reported in one of the studies that originally characterized this gene (named *FBX* therein) [14]. The FBXO7 mRNA appeared to be broadly expressed in human tissues, but enriched in bone marrow, liver, kidney, testis, and thyroid gland. Interestingly, a strong expression was also found in several regions of the human brain, such as the corpus callosum, caudate nucleus, substantia nigra, as well as in the spinal cord [14]. Furthermore, microarray data on the regional expression of the *FBXO7* gene in the human brain, are available in the ALLEN Human Brain Atlas website (http://www.brain-map.org, accessed on Dec. 1, 2010). In this Atlas, *FBXO7* expression levels are high in the cerebral cortex (particularly the frontal and parietal regions), the striatum, pallidum, thalamus, substantia nigra, red nucleus, and deep cerebellar nuclei, while low expression levels are documented in the hippocampus and the cerebellar cortex.

The *FBXO7* mRNA and proteins seem therefore highly expressed in the motor areas of the human brain, including both the extrapyramidal and the pyramidal systems, which fits with the clinical phenotype of parkinsonian-pyramidal disorder caused by the loss of the FBXO7 function in PARK15. Intriguingly, the widespread and abundant expression of the FBXO7 proteins in the frontal cerebral cortex suggests that additional, cognitive and behavioural disturbances of frontal type might be prominent in the phenotype. Interestingly, severe behavioural disturbances were noted in one of the Dutch PARK15 patients [10].

In conclusion, the common cellular abnormality found in the PARK15 patients from the Dutch and Italian families is the depletion of the FBXO7 isoform 1, which normally localizes mostly in the cell nucleus. The activity of FBXO7 in the nucleus appears therefore crucial for the maintenance of brain neurons and the pathogenesis of PARK15.

Materials and Methods

Ethics Statement

The study was approved by the Medical Ethical Committee (Medisch Ethische Toetsings Commissie, METC) of the Erasmus MC Rotterdam, and all participating subjects provided their informed consent.

Subjects

The Dutch and Italian families with *FBXO7* mutations have been described previously by some of us [10].

Cell culture and transfection

Lymphoblastoid cell lines were obtained by Epstein-Barr virus (EBV) immortalization of peripheral blood cells obtained from patients and controls, according to standard protocols. The lymphoblastoid cells were cultured in RPMI 1640 medium (Gibco) supplemented with 15% fetal calf serum, 50 U/ml penicillin and 50 mg/ml streptomycin, in a humidified 5% CO_2 incubator. Human Embryonic Kidney (HEK) 293T cells, human neuroblastoma cells (SH-SY5Y), and human fibroblasts were grown in Dulbecco's modified Eagle's medium (DMEM) (Lonza). The HEK 293T cells were incubated in a humidified 5% CO_2 incubator, and the SH-SY5Y cells and fibroblasts were incubated in a humidified 10% CO_2 incubator. The HEK 293T cells were transiently transfected by polyethyleneimine (PEI, Polysciences Inc.). Lipofectamine^{TM} LTX and PLUS^{TM} Reagents (Invitrogen) transfection were used in SH-SY5Y cells according to the manufacturer's instructions. Furthermore, stable *FBXO7* knock down HEK 293T cells were generated using *FBXO7* shRNA (#TRCN 0000004339, Sigma); a non-targeting vector (shNT) (SHC002, Sigma) was used as control. Mouse primary hippocampal neurons were dissected and cultured as described previously [23]. After 20 days *in vitro*, the hippocampal neurons were transfected with constructs expressing wild type or mutant FBXO7 by using Lipofectamine 2000 (Invitrogen).

FBXO7 constructs

The full-length *FBXO7* cDNA (GenBank accession number NM_012179.3; NP_036311.3) was amplified by PCR using cDNA obtained from SH-SY5Y neuroblastoma cells as template. The PCR product was ligated into pcDNA^{TM}3.1/V5-His-TOPO (Invitrogen). After sequencing, the insert WT *FBXO7* was subcloned in frame into the mammalian expression plasmid pEGFP-C3 (BD biosciences), resulting in an N-terminal fusion protein eGFP-FBXO7. All primers used are given in the Supplementary Table S1. The untagged WT *FBXO7* was obtained using the QuikChange site-directed mutagenesis kit (Stratagene) by introducing a stop codon in front of the V5-His tag. All untagged *FBXO7* mutants (T22M, R378G, and R498X) were also prepared using the above-mentioned mutagenesis kit. The cDNA fragment encoding the first 40 amino acids of WT or T22M-mutant FBXO7 isoform 1 was amplified and subcloned in front of mCherry-labeled profilin (the mCherry-profilin construct was a gift from Josien Levenga, Clinical Genetics Department, Erasmus MC). The complete cDNA open reading frame of all constructs was verified by direct sequencing.

Immunofluorescence

The HEK 293T and SH-SY5Y cells were seeded onto glass coverslips coated with 0.1% gelatin (Sigma-Aldrich), and transfected with untagged WT or mutant *FBXO7* constructs. The cells were fixed in 4% (w/v) paraformaldehyde in PBS for 10 minutes and permeabilized in 100% methanol for 20 minutes. The cells were then blocked with 3% bovine serum albumin (BSA, Sigma) in PBS (w/v) for 30 minutes, and probed at 4°C overnight with mouse polyclonal antibody raised against full-length FBXO7 (Abnova, 1/300). The samples were then incubated with Cy3-coupled secondary anti-mouse antibodies (Jackson ImmunoResearch, 1/200) for 1 hour. The cell nuclei were stained with Hoechst dye 33342 (Invitrogen), but the staining is shown in green color to increase image contrast. Cells were then mounted on slides with fluorescent mounting medium (DAKO). Fluorescence images were collected using a Leica SP5 confocal microscope (Leica Microsystems), and analyzed with the Leica Confocal Software.

Immunofluorescence of primary hippocampal neurons was performed 24 hours after transfection. The cells were fixed with 4% paraformaldehyde and permeabilized with staining buffer containing 50 mM Tris, 0.9% NaCl, 0.25% gelatin, and 0.5% Triton X-100, at pH 7.4. The subsequent antibody incubation was performed as described above.

Quantitative PCR (qPCR)

Total RNA was isolated by RNA Bee (TEL-TEST Inc.) from EBV-transformed lymphoblastoid cells and converted into first-strand cDNA using the iScript^{TM} cDNA Synthesis Kit (Bio-Rad). qPCR was carried out using a KAPA SYBR® FAST qPCR Kit (Kapa Biosystems) in the ABI Prism 7300 Sequence Detection System (Applied Biosystems). Thermal cycling conditions in the ABI Prism 7300 Detection System were as follows: denaturing step (95°C for 3 minutes), followed by 35 cycles of denaturing (95°C for 5 seconds), annealing and extension (60°C for 30 seconds). Fluorescence detection and data analysis were performed by ABI Prism 7300 SDS software (version 1.3.1, Applied Biosystems). Experiments were performed in triplicate using hypoxanthine phosphoribosyltransferase (HPRT) as the endogenous control for gene expression normalization.

The primers used for the qPCR studies, including one assay for the total *FBXO7* transcripts (isoform 1 and isoform 2), one assay specific for the isoform 1, and another assay specific for the isoform 2, are given in Supplementary Table S2.

Western Blotting

The cells were washed with cold phosphate buffer (PBS) and harvested in lysis buffer containing 20mM Tris-HCl at pH 8.0, 150mM NaCl, 1mM $NaVO_4$, 50mM NaF, 1% Triton X-100, and a protease inhibitor cocktail (Roche Molecular Biochemicals). The cells were lysed for 30 minutes on ice before centrifugation (15000 *g* for 10 minutes at 4°C), and then the total protein concentration of the supernatant was determined by using the

bicinchoninic acid (BCA™) protein assay kit (Pierce) according to the manufacturer's instructions. The protein samples (40 micrograms) were separated by 6%–12% Criterion™ XT 4–12% Bis-Tris Gel (Bio-Rad), and then transferred to nitrocellulose membranes. Membranes were blocked with 5% low-fat milk powder (Fluka) in 1×PBS containing 0.1% Tween20 (PBST) for 1 hour at room temperature and incubated overnight at 4°C with mouse polyclonal antibody against full length FBXO7 (Abnova, 1/3000) and mouse monoclonal against actin (Abcam, 1/2500) or against eGFP (Roche, 1/2000). After washing 3 times with PBST, the membranes were incubated in the dark for 1 hour with PBST containing donkey anti-mouse secondary antibodies (800nm, LI-COR Biosciences Lincoln, 1/5000 dilution). After washing, the membranes were scanned using the Odyssey™ Infrared Imager (Li-COR Biosciences). The integrated intensities of the protein bands were quantified by the Odyssey software.

Proteasome and lysosomal-mediated degradation of FBXO7 mutants

The HEK 293T cells were seeded onto 6-well plates and transfected with 1.5 µg *FBXO7* constructs; empty vector pcDNA3 (Invitrogen, Carlsbad, CA, U.S.A.) was used as mock control. To test for the proteasomal degradation of the FBXO7 protein, 40 hours after transfection the cultured medium was replaced with DMEM containing either 42 µM MG-132 (Sigma-Aldrich) or vehicle control DMSO. After 6 hours incubation, the cells were harvested and analyzed by WB. The lysosomal degradation pathway was tested by adding 30mM NH_4Cl to the cell culture 28 hours after transfection. The cells were incubated with NH_4Cl for 20 hours and harvested for WB analysis.

FBXO7 protein studies in human brain tissue

Human brain tissues were obtained from The Netherlands Brain Bank, Netherlands Institute for Neuroscience, Amsterdam. All material has been collected from donors from whom a written informed consent for brain autopsy and the use of the material and clinical information for research purposes had been obtained by the Netherlands Brain Bank. For immunohistochemistry, paraffin-embedded sections (7 µm) were analyzed from the brain of two non-parkinsonian, non-demented male donors (age at death 76 and 81 years-old). The following regions were studied: frontal, temporal, and occipital cerebral cortex, globus pallidum, hippocampus, substantia nigra, and cerebellum. Briefly, dewaxed sections were pretreated for antigen retrieval using pressure cooking in 0.1 M sodium citrate buffer (pH 6) for 5 min. Subsequently, sections were incubated overnight with antibodies against FBXO7 (Abnova, 1:100) at 4°C. The broad spectrum poly-AP powervision reagent (immunoLogic) was used for 1 hour at room temperature for visualization. Enzyme detection was performed by using 1% new fuchsin, 1% sodiumnitrite, 0.03% naphtol AS-MX phosphate (Sigma), and 0.025% levamisol (Acros) for 20 minutes at room temperature. The sections were not counterstained but directly mounted in aquamount for examination under a light microscope.

Data analysis and statistics

Quantitative data are expressed as means ± SEM based on at least three independent experiments. Statistical analyses were performed using contingency tables.

Supporting Information

Figure S1 Validation of the specificity of the FBXO7 antibody by Western blotting in stable *FBXO7* gene knock down HEK 293T cells.
(PDF)

Figure S2 Validation of the specificity of the FBXO7 antibody by immunofluorescence in stable *FBXO7* gene knock down HEK 293T cells.
(PDF)

Figure S3 qPCR analysis of *FBXO7* isoform-specific transcripts in members of the PARK15 families and unrelated healthy controls (C1–C3).
(PDF)

Figure S4 Overexpression of wild type and mutant FBXO7.
(PDF)

Figure S5 Positively charged amino acids in the FBXO7 protein.
(PDF)

Table S1 Primers used for molecular cloning.
(PDF)

Table S2 Primers used for qPCR.
(PDF)

Acknowledgments

We thank the family members for their participation, Dr. Mark Nellist and Dr. Andre Hoogeveen (Dept. Clinical Genetics, Erasmus MC, Rotterdam) for their helpful advices, and Tom de Vries Lentsch for artwork.

Author Contributions

Conceived and designed the experiments: TZ EDG BAO VB. Performed the experiments: TZ EDG GJB AL LAS. Analyzed the data: TZ EDG GJB RW VB. Contributed reagents/materials/analysis tools: CHW FWV MCJD PM. Wrote the paper: TZ VB. Revised the paper for important intellectual content: EDG BAO.

References

1. Tolosa E, Wenning G, Poewe W (2006) The diagnosis of Parkinson's disease. Lancet Neurol 5: 75–86.
2. Gupta A, Dawson VL, Dawson TM (2008) What causes cell death in Parkinson's disease? Ann Neurol 64 Suppl 2: S3–15.
3. Gasser T (2009) Molecular pathogenesis of Parkinson disease: insights from genetic studies. Expert Rev Mol Med 11: e22.
4. Bonifati V (2007) Genetics of parkinsonism. Parkinsonism Relat Disord 13 (Suppl 3): S233–S241.
5. Healy DG, Falchi M, O'Sullivan SS, Bonifati V, Durr A, et al. (2008) Phenotype, genotype, and worldwide genetic penetrance of LRRK2-associated Parkinson's disease: a case-control study. Lancet Neurol 7: 583–590.
6. Ahlskog JE (2009) Parkin and PINK1 parkinsonism may represent nigral mitochondrial cytopathies distinct from Lewy body Parkinson's disease. Parkinsonism Relat Disord 15: 721–727.
7. Bonifati V (2010) PARK7, DJ1. In: Kompoliti K, Verhagen Metman L, eds. Encyclopedia of Movement Disorders. Oxford: Academic Press 3: 392–395.
8. Ramirez A, Heimbach A, Grundemann J, Stiller B, Hampshire D, et al. (2006) Hereditary parkinsonism with dementia is caused by mutations in ATP13A2, encoding a lysosomal type 5 P-type ATPase. Nat Genet 38: 1184–1191.
9. Gitler AD, Chesi A, Geddie ML, Strathearn KE, Hamamichi S, et al. (2009) Alpha-synuclein is part of a diverse and highly conserved interaction network that includes PARK9 and manganese toxicity. Nat Genet 41: 308–315.
10. Di Fonzo A, Dekker MC, Montagna P, Baruzzi A, Yonova EH, et al. (2009) FBXO7 mutations cause autosomal recessive, early-onset parkinsonian-pyramidal syndrome. Neurology 72: 240–245.
11. Shojaee S, Sina F, Banihosseini SS, Kazemi MH, Kalhor R, et al. (2008) Genome-wide linkage analysis of a Parkinsonian-pyramidal syndrome pedigree by 500 K SNP arrays. Am J Hum Genet 82: 1375–1384.
12. Cenciarelli C, Chiaur DS, Guardavaccaro D, Parks W, Vidal M, et al. (1999) Identification of a family of human F-box proteins. Curr Biol 9: 1177–1179.
13. Winston JT, Koepp DM, Zhu C, Elledge SJ, Harper JW (1999) A family of mammalian F-box proteins. Curr Biol 9: 1180–1182.

14. Ilyin GP, Rialland M, Pigeon C, Guguen-Guillouzo C (2000) cDNA cloning and expression analysis of new members of the mammalian F-box protein family. Genomics 67: 40–47.
15. Ho MS, Ou C, Chan YR, Chien CT, Pi H (2008) The utility F-box for protein destruction. Cell Mol Life Sci 65: 1977–2000.
16. Kirk R, Laman H, Knowles PP, Murray-Rust J, Lomonosov M, et al. (2008) Structure of a Conserved Dimerization Domain within the F-box Protein Fbxo7 and the PI31 Proteasome Inhibitor. J Biol Chem 283: 22325–22335.
17. Hsu JM, Lee YC, Yu CT, Huang CY (2004) Fbx7 functions in the SCF complex regulating Cdk1-cyclin B-phosphorylated hepatoma up-regulated protein (HURP) proteolysis by a proline-rich region. J Biol Chem 279: 32592–32602.
18. Chang YF, Cheng CM, Chang LK, Jong YJ, Yuo CY (2006) The F-box protein Fbxo7 interacts with human inhibitor of apoptosis protein cIAP1 and promotes cIAP1 ubiquitination. Biochem Biophys Res Commun 342: 1022–1026.
19. Laman H, Funes JM, Ye H, Henderson S, Galinanes-Garcia L, et al. (2005) Transforming activity of Fbxo7 is mediated specifically through regulation of cyclin D/cdk6. Embo J 24: 3104–3116.
20. Holbrook JA, Neu-Yilik G, Hentze MW, Kulozik AE (2004) Nonsense-mediated decay approaches the clinic. Nat Genet 36: 801–808.
21. Boulikas T (1994) Putative nuclear localization signals (NLS) in protein transcription factors. J Cell Biochem 55: 32–58.
22. French CA, Tambini CE, Thacker J (2003) Identification of functional domains in the RAD51L2 (RAD51C) protein and its requirement for gene conversion. J Biol Chem 278: 45445–45450.
23. Levenga J, Buijsen RA, Rife M, Moine H, Nelson DL, et al. (2009) Ultrastructural analysis of the functional domains in FMRP using primary hippocampal mouse neurons. Neurobiol Dis 35: 241–250.